STRUT-AND-TIE MODEL FOR PUNCHING SHEAR OF CONCRETE SLABS

RICHARD W. TILLER

STRUT-AND-TIE MODEL FOR PUNCHING SHEAR OF CONCRETE SLABS

by

Richard W. Tiller, B. Eng.

A thesis submitted to the School of Graduate Studies in partial fulfilment of the requirements for the degree of Master of Engineering

Faculty of Engineering and Applied Science
Memorial University of Newfoundland
August 1995

St. John's Newfoundland Canada

ISBN 0-612-06151-5

Canada

"The concept also incorporates the major elements of what is today called detailing and replaces empirical procedures, rules of thumb and guess work by a rational design method. Strut-and-tie models could lead to a clearer understanding of the behaviour of structural concrete and codes based on such an approach would lead to improved structures."

- Schlaich, Schafer, Jennewein, 1987

To Michael, who blessed us with his arrival sometime in Chapter 2.

ABSTRACT

The reinforced concrete slab system is an economical and popular structural slab system in building and offshore construction. A major concern of this system is localized punching shear failure at the slab-column interface. Punching shear failure occurs when the column "punches" through the slab. This type of failure is unpredictable and often sudden resulting in cathastrophic failure of the slab system.

Current North American design codes deal with punching shear in an empirical equation based mainly on test results. This approach is limited to concrete with a compressive strength generally less than 40 MPa. The strut-and-tie method considers the flow of forces in a reinforced concrete element to consist of a series of compressive struts and tension ties joined at nodes. The strut-and-tie method is a rational approach to structural concrete design which results in a uniform and consistent design philosophy.

A strut-and-tie model has been developed to model the punching shear behaviour of a concrete slab. This model provides a quick and simple approach to punching shear behaviour. It is applicable for both normal and high strength concrete under symmetric and nonsymmetric loading with and without shear reinforcement.

The strut-and-tie model for symmetric punching consists of a "bottle shaped" compressive zone in the upper section of the slab depth leading to a "parallel stress" compressive zone in the lower section depth. Inclined shear cracking develops in the bottle shaped zone prior to failure in the lower zone. Cracking in the bottle shaped zone is related to the diagonal tensile strength of the concrete. Ultimate punching failure occurs in the parallel stress zone by a high radial compressive stress failure. An equation based failure criteria for the strut-and-tie method is used to model the behaviour in the lower compressive stress zone. The results of the strut-and-tie model

for symmetric punching shear behaviour were compared to experimental test results performed and published by others. The results of the strut-and-tie model showed excellent agreement with these test results.

A strut-and-tie model was also developed to rationally model nonsymmetric punching shear behaviour due to unbalanced moment transfer and symmetric punching behaviour of concrete slabs with shear reinforcement. These models showed excellent agreement with test results performed and published by others.

The strut-and-tie method presents a unified, consistent, rational behaviour model for structural concrete elements including the punching shear phenomena of concrete slabs.

ACKNOWLEDGEMENTS

This thesis was completed at the Faculty of Engineering and Applied Science at Memorial University of Newfoundland in St. John's, Newfoundland, Canada.

I would like to thank Dr. H. Marzouk, Professor of Civil Engineering under whose supervision this thesis project was carried out. My masters program was conducted on a part-time basis as I worked in the Consulting Engineering field. I would like to thank my employers, BFL Consultants Ltd. and Structural Consultants Ltd. for their understanding and assistance. I would also like to thank my academic colleague, Amgad Hussein, M. Eng., whose work with Dr. Marzouk initiated this report.

I would also like to thank my wife, Susan, for her encouragement during this project.

Contents

List of Tables

List of Figures

List of Symbols

A_s	area of reinforcing steel
A_{sr}	area of the reinforcing steel in the radial direction
A_{st}	area of the reinforcing steel in the tangential direction
B	diameter of equivalent circular column
C	compression force
E_c	modulus of elasticity of concrete
E_s	modulus of elasticity of reinforcing steel
F_{cr}	radial concrete force
F_{ct}	tangential concrete force
F_{sr}	radial reinforcing steel force
F_{st}	tangential reinforcing steel force
M_r (Mult)	bending capacity of slab (bending moment resistance)
P	concentrated load
P_{eq}	equivalent concentrated load
$Pult.$	ultimate shear capacity

P_{test} ultimate test load

R_0 resultant force

STM strut-and-tie model

T oblique compressive force in the imaginary conical shell assumed by Kinnunen and Nylander, tension force of strut-and-tie model

V_a calculated punching shear capacity for high radial compression stress failure mechanism

V_r calculated punching shear capacity for high tangential compression strain failure mechanism

V_f applied shear force of slab (factored)

a side dimension of a square column

b perimeter of the loaded area

c side dimension of a square column

d slab effective depth

e eccentricity of shear force

f_{bu} limiting bearing strength

f'_c compressive cylinder strength of concrete

f_{ce} compressive strut stress in strut-and-tie model

f_{cu} cube concrete strength

f'_r modulus of rupture

f_t concrete tensile strength

f_y	yield strength of reinforced steel
f_2	concrete compressive stress in strut-and-tie model
f_{c2} max	reduced concrete compressive stress in strut-and-tie model
h	slab overall depth
k	factor
m	unit moment capacity
$n = E_s/E_c$	modular ratio
q	applied load
r_0	radius of column or loaded area
r_p	radius to the loading
r_u	radius of punch
r_y	radius within which all flexural reinforcement yield
r_3	radius of a slab
s	side dimension of slab specimen
t	thickness of member
v_u	nominal shear capacity
w, w_s	width of compressive stress field
x	neutral axis depth
x_{pu}	height of compression zone at flexure in tangential direction

z, jd lever arm

y distance from extreme compressive fibre to neutral axis

α angle of inclination of the concrete force at the column face

ϵ_c concrete strain

ϵ_{c1} $0.85\ f'_c/4700\sqrt{f'_c}$

ϵ_{ct} concrete tangential strain

ϵ_{cu} concrete ultimate strain

ϵ_{cpu} critical concrete punching strain

ϵ_{st} steel tangential strain

ϵ_{sy} yield strain of reinforcing steel

ϵ_s steel strain

ϵ_1 principle tensile strain

ρ reinforcement ratio (A_s/bd)

ρ_r ratio of radial reinforcement

ρ_t ratio of tangential reinforcement

Φ_o P_u/P_{flex}

$\Delta\Phi$ small sectorial angle of a radial segment

Ψ rotation of the slab portion outside the shear crack

Ψ_f rotation at failure

σ_1 maximum compressive principle stress

σ_2 minimum compressive principle stress

Θ_0 spreading angle in strut-and-tie model

ϕ_c, ϕ_s material resistance factors

μ bond stress

Chapter 1

Introduction

The reinforced concrete slab system is an economical and popular structural system in building and offshore construction. A major concern of this system is localized punching shear failure at the slab-column location. The catastrophic nature of punching shear failure has been a major concern for engineers for many years.

Current North American codes (ACI 318 [52] and CSA CAN3-A23.3 [53]) deal with punching shear using an empirical equation based mainly on test results from Moe [1]. This approach does not rationally model the actual slab-column behaviour and is limited to slabs of relatively low compressive strength, 14-40 Mpa. Hence, it is necessary to develop a rational model to predict the behaviour and ultimate shear capacity of concrete slabs of varying compressive strengths. The strut-and-tie model, considers the flow of forces within a structural element to consist of a series of compressive struts and tension ties joined at nodes, is proposed to rationally model this situation.

1.1 Scope

A strut-and-tie model, based on an elastic theory and on the classical Kinnunen and Nylander plate theory model [13], was developed to model the behaviour and ultimate punching shear capacity of both normal strength and high strength concrete slabs for

symmetric and nonsymmetric punching shear. Slabs with shear reinforcement were also considered under symmetric loading. The strut-and-tie models were compared to experimental test results reported in past literature and current Canadian code requirements. A computer spreadsheet program called "PUNCH" was developed to assist in the calculations involved with modelling these punching shear situations, see Appendix A.

1.2 Objectives

The main objectives of this thesis are:

1. To examine the structural behaviour of punching shear in concrete slabs.
2. To examine the application of strut-and-tie models in structural concrete elements.
3. To develop a rational strut-and-tie model to predict the behaviour and ultimate punching shear of normal and high strength concrete slabs. The model includes symmetric and nonsymmetric loading and punching shear reinforcement.

1.3 Thesis Outline

Chapter 2 reviews past literature conducted on punching shear of concrete slabs including empirical and rational studies and present North American design codes requirements.

Chapter 3 reviews the concept of the strut-and-tie model. It deals with its basic components, general design procedures, and some examples of applications.

Chapter 4 describes the proposed components of a strut-and-tie model to describe punching shear behaviour in concrete slab systems.

Chapter 5 compares the punching shear behaviour of a slab using the strut-and-tie method to published experimental test results and the current Canadian concrete code.

Chapter 6 describes the conclusions reached in this investigation.

mainly to diagonal tension in the concrete. Hence, v should be proportional to the concrete tensile strength, f_t. This equation contradicts experimental findings since as the reinforcement ratio increases the predicted punching shear decreases.

Graf [4] reported the results of an experimental study on slabs subjected to concentrated loads in 1938. This was followed by the work of Forsell and Holemberg [5] in 1946. Their formulation was similar to that of Talbot's except for the location of the critical section. According to Graf [4], the critical section was at the column periphery, while Forsell and Holemberg located the critical section at a distance $h/2$ from the column face. In the latter case, the shear stress distribution is assumed to be parabolic over the slab thickness:

$$v = \frac{V}{4ch} \tag{2.2}$$

$$v = \frac{V}{4(c+\frac{h}{2})h}. \tag{2.3}$$

Hognestad [6], in 1953, was the first to propose a design equation in which the influence of flexural strength on the ultimate shear stress was taken into account. After a re-evaluation of Richart's [7] tests on column footings, Hognestad [6] showed that the design methods of the time (based on Equation 2.1) did not give a consistent factor of safety with respect to shearing failures. It was suggested that the ultimate punching shear is mainly dependent upon the following variables:

1. Properties of the materials used in the slab:
   (a) concrete cylinder strength, f'_c;
   (b) amount, type, and grade of tension and compression reinforcement.
2. Size and shape of the loaded area in relation to the slab thickness.
3. Span, support condition, and edge restraints of the slab.

Hognestad [6] concluded that the ultimate shearing stress of a variety of slabs could be expressed by the empirical equation:

$$v = \left(0.035 + \frac{0.07}{\Phi_0}\right) f'_c + 130 \qquad \text{psi} \tag{2.4}$$

where Φ_0 is the ratio of the ultimate shearing capacity of the slab to the ultimate flexural capacity of the slab if it had not failed in shear. The ultimate flexural capacity of the slab was computed using yield line theory and was dependent on the properties of the slab and the size and position of the loaded area. Hognestad conceded that Equation 2.4 might not be valid for slabs with dimensional ratios or concrete strengths outside the ranges of those of Richart's slabs.

Elstner and Hognestad [8] reported in 1952 shear tests of a further 24 slabs. Equation 2.4 was reviewed in the light of these tests and those reported by Forsell and Holemberg [5] and Richart and Kluge [9]. Satisfactory agreements between observed and predicted shearing failure loads were found to exist.

Additional tests were performed in order to extend the ranges of the slab variables of previous test programmes. Elstner and Hognestad [10], in 1956, reported that Equation 2.4 gave unsafe estimates of the ultimate punching shear strength of slabs of high-strength concrete. The following equation was found to be in better agreement with the test results.

$$v = \frac{0.046}{\Phi_0} f'_c + 333 \qquad \text{psi} \tag{2.5}$$

It was also reported that neither a concentration of tension reinforcement directly beneath the loaded area nor the presence of compression reinforcement had any appreciable effect on the ultimate punching shearing strengths of the concrete slabs tested.

Moe [1] conducted an experimental investigation consisting of five different series of test slab and studying the effect of:

1. Casting holes in the slab in the column vicinity.

2. Concentrating the tensile reinforcement over the column.

3. Including special types of shear reinforcement.

4. Extreme column size.

5. Eccentric column loads or transfer of moment.

Moe, based on his experimental program, developed a semi-empirical type equation to calculate the ultimate punching shear strength:

$$v_u = \frac{P_u}{cd} = \frac{15(1 - \frac{0.075}{d})\sqrt{f'_c}}{1 + \frac{5.25bd\sqrt{f'_c}}{P_{flex}}} \quad \text{psi} \tag{2.6}$$

Moe stated that the critical section of a slab, subjected to a concentrated load, was at the column perimeter and that the shear strength was to some extent dependent upon the flexural strength.

In the report of ACI-ASCE Committee 326 [12] of 1962, the recommendations of the existing concrete building code were reviewed in the light of the research carried out at that time. It was suggested that Moe's equation (Equation 2.6) was the best equation to date for the prediction of the punching failure load of slabs tested under laboratory conditions. For practical design, Φ_0 was eliminated from Moe's equation by assuming that it was equal to unity. Following Moe's suggestion that the punching shearing strength is a function of the square root of the concrete compressive strength, the Committee recommended that the following classical design equation for the calculations of the ultimate shear load:

$$V = vbd \tag{2.7}$$

where $v \leq 4.0\sqrt{f'_c}$ - (psi) and b is the length of the "pseudo critical section," taken as the perimeter at a distance of $d/2$ from the periphery of the loaded area. The position of the assumed critical section was chosen so that Equation 2.7 incorporates allowance for the c/d ratio.

2.1.3 Rational Studies

Kinnunen and Nylander [13], based on observations of a number of tests of circular slabs with central columns, conceived an idealized model of a slab at punching failure. It was assumed that the slab portion outside the shear crack, which is bounded by this crack, by radial cracks, and by the circumference of the slab, can be regarded as a rigid body which is rotated under the action of the load around a centre of rotation located at the root of the shear crack. The model is illustrated in Figures 2.1 and 2.2.

The criterion of failure in the mechanical model was the collapse of the conical shell which occurred when the tangential strain on the surface of the slab in the vicinity of the root of shear crack reached an empirical critical value. The characteristic tangential strain at failure was determined from tests on slabs with ring reinforcement only. The punching load was calculated by assuming a dimension of the conical shell and then following a convergent iterative process.

Kinnunen and Nylander found that their theory gave values for the punching load which were in satisfactory agreement with results of their own tests as well as those of Elstner and Hognestad [10]. They attributed low calculated values, in the case of two-way reinforcement, to dowel and membrane effects, and suggested that they should be taken into account by multiplying the calculated ultimate load by 1.1.

Kinnunen [14] later published a paper in which he presented a primarily qualitative study of dowel and membrane action in slabs with two-way reinforcement and

a)

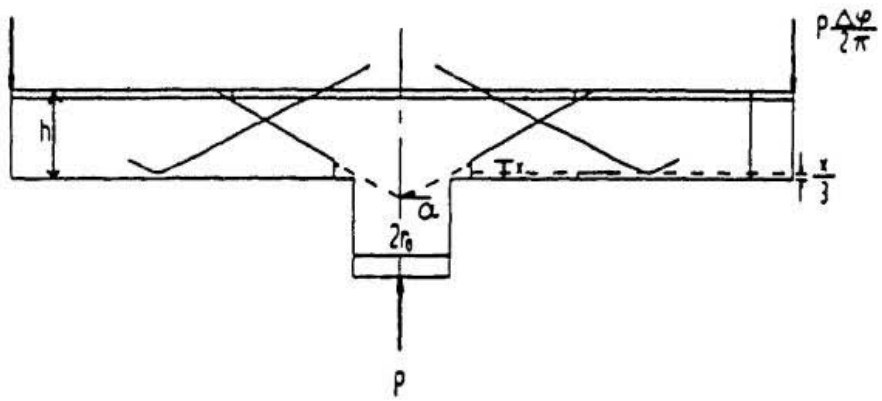

Figure 2.1: Punching shear model by Kinnunen and Nylander.

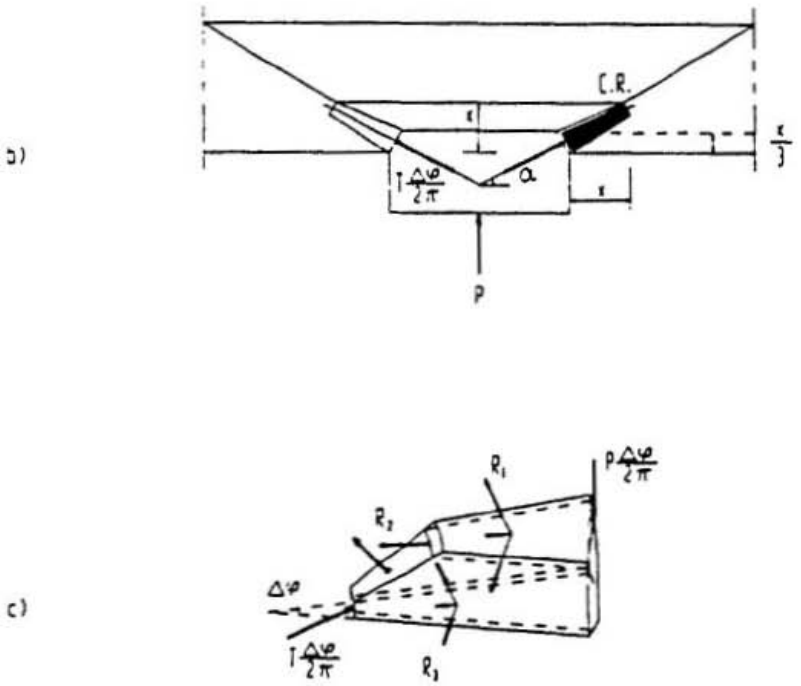

Figure 2.2: Punching model adopted by Kinnunen and Nylander.

concluded that the punching load is increasing by about 20 per cent by dowel and membrane effects.

The Kinnunen and Nylander model was later criticized by Long [15] and Reimann [16]. Their major common objection was that the assumption that the compressive strength in the conical shell was approximately constant throughout and was made in neglect of probable shearing stresses on the shell surface.

This criticism implies that the existence of the assumed conical shell should have been proven. Rather than verifying its existence, Kinnunen and Nylander have justified its use, along with that of their criterion of failure. by showing consistent satisfactory agreement between calculated and test punching loads.

Based on the test observations of Kinnunen and Nylander [13]. Reimann [16] proposed a simple idealised model of slab at punching failure from which the punching load can be calculated directly. The theoretical model is made up of a punched cone of concrete, an outer annular slab and a joint, which was idealized as a hinge bridged by a spring, between the inner and outer regions at the periphery of the column. The hinge was assumed to coincide with the centre of rotation of the annular slab. The model is illustrated in Figure 2.3. Reimann applied his method of analysis to results of tests by Kinnunen and Nylander and others. He found reasonable agreement between calculated and test failure loads although the average values of the ratio of the actual failure load to his calculated failure loads were usually greater than unity. Reimann ignored any dowel and tensile membrane effects which could account for his somewhat low calculated values.

In 1967, Long [15] and Long and Bond [17] reported a theoretical method for the calculation of the punching shear load of a slab with two-way reinforcement. Assuming a linear distribution of stress, the stresses in the shear-compression zone were calculated using thin plate theory. An octahedral shear stress criterion of failure was

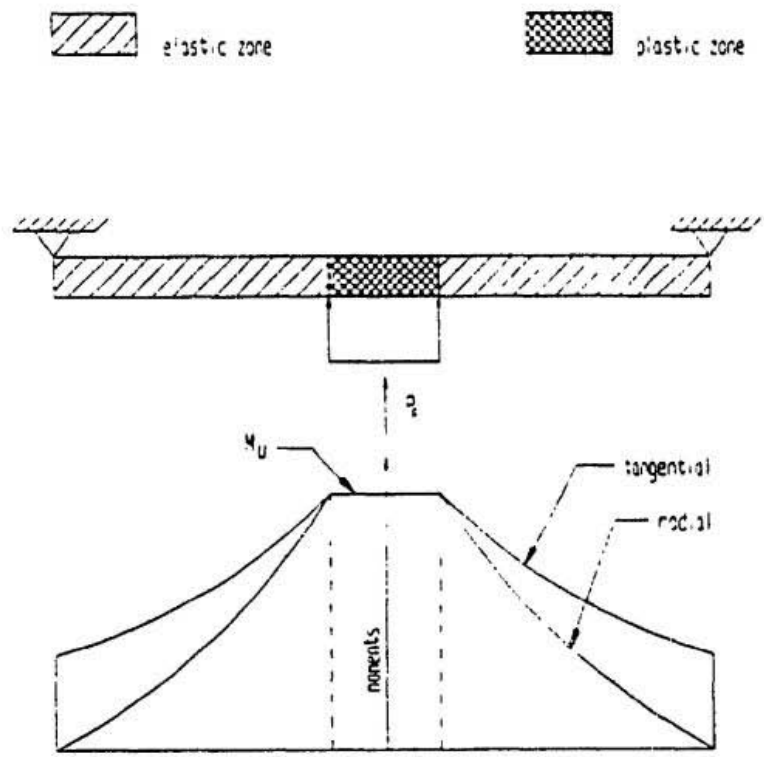

Figure 2.3: The Mechanical model proposed by Reimann.

used to find the stresses at failure and from that an uncorrected load was calculated. The uncorrected load was then adjusted to give the punching load by applying corrections for surrounding slab and support conditions and for dowel and tensile membrane effects.

Long and Bond showed that their theory gave punching loads in good agreement with test results of, among others, Richart, Elstner and Hognestad, Moe, and Kinnunen and Nylander.

In the discussion which followed this work, the relevance of the equations of elasticity to slabs near failure and the suggested mechanism of punching failure was questioned. The assumption of Long and Bond that the load supported by a failed slab approximates the effect of dowel and tensile membrane action on the failure load is also questionable.

Masterson and Long [18] proposed a simplified finite element model for local slab conditions at ultimate failure. Their idealized representation of the slab-column connection was equivalent to the theory of development of local plasticity at the column periphery. By relating the applied load to the internal moment at failure and by making an appropriate allowance for dowel and membrane effects, the punching strength was found to be well-predicted for the majority of chosen realistic slab-column specimens tested by some researchers.

Long [19] later formulated a two-phase design procedure in which the punching strength was predicted as the lesser of either a flexure or shear criterion of failure. This approach has certain limitations, as it could not handle slabs with high-strength concrete and slabs with low levels of reinforcement.

In 1987, Long [20] extended his work by using a more rational treatment of the flexural mode of punching failure. Long used an analytically based linear interpolation moment factor to relate the ultimate flexural capacity to the yield moment. This

factor depended on the slab ductility which was considered to control the degree of yielding in the slab at failure. The ultimate shear capacity was based on an empirical relationship for vertical shear stress on a critical section close to the column perimeter.

In 1970, Gesund and Dikshit [21] used yield line theory of Johansen (1962) to analyze punching failures in slabs. Their work was based on the research carried out by Gesund and Kaushik [22] who concluded that the ratio P_{flex}/P_{test} for 106 alleged punching shear failures averaged 1.015 with a standard deviation of 0.248. They assumed a yield line fan mechanism around the column, as shown in Figure 2.4. The ultimate load calculated for that mechanism was considered to be the ultimate punching load for the case of an interior circular column. This method overestimates the punching strength unless the flexural mode of failure is the dominant one.

Another application of plastic theory to estimate the punching resistance of axisymmetric concrete slabs without shear reinforcement was presented by Nielsen, Braestrup et al. [23] in 1978. This theory is in contrast with Gesund's method, as the punching mechanism adopted in Figure 2.5 is totally independent of the flexural properties of the slab. The mechanism is one of the punching of a solid of revolution attached to the column, while the rest of the slab remains rigid. Using minimization of work, together with the modified Coulomb criterion, see Figure 2.6, the minimum upper bound solution for the ultimate punching load was obtained. This theory contradicts experimental findings as it neglects the effect of the flexural reinforcement on the ultimate punching capacity of the slab.

In 1982, Andrä [24] presented a theoretical model for the punching shear of a circular slab with ring reinforcement. A finite element analysis was used to derive the proposed model. As done by Kinnunen and Nylander, the model considers the rigid body rotation of radial segments around a center of rotation located at the face of the column and the neutral axis, as shown in Figure 2.7. Each segment is analyzed using

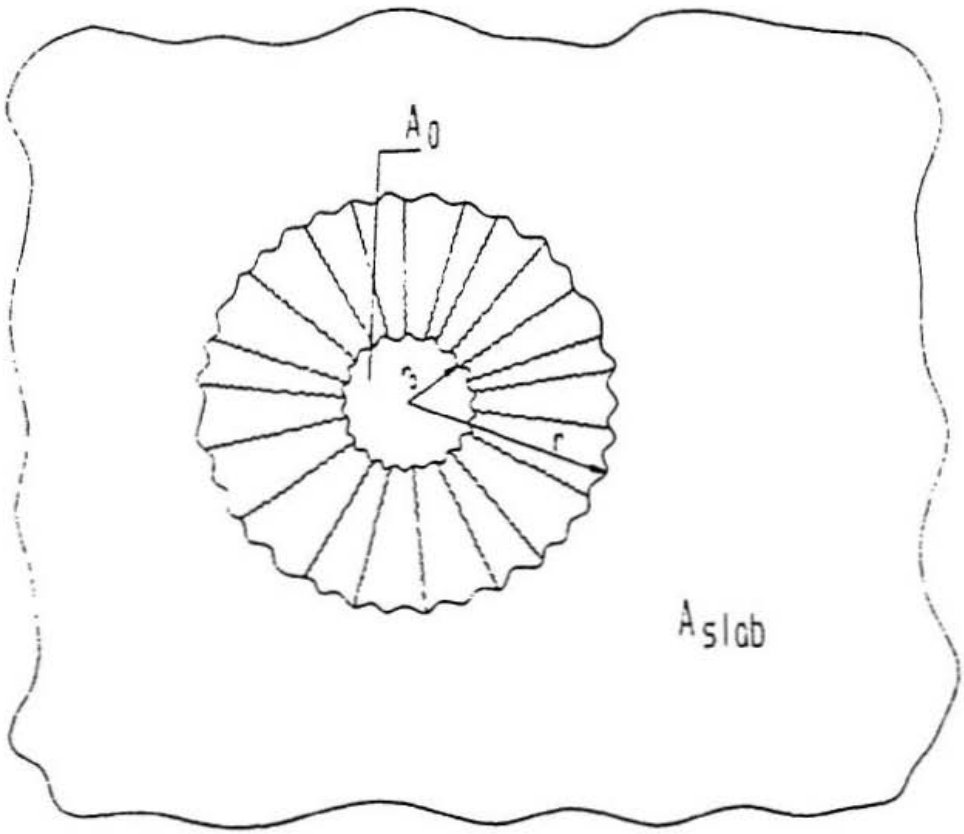

Figure 2.4: Yield line mechanism used by Gesund *et al.*

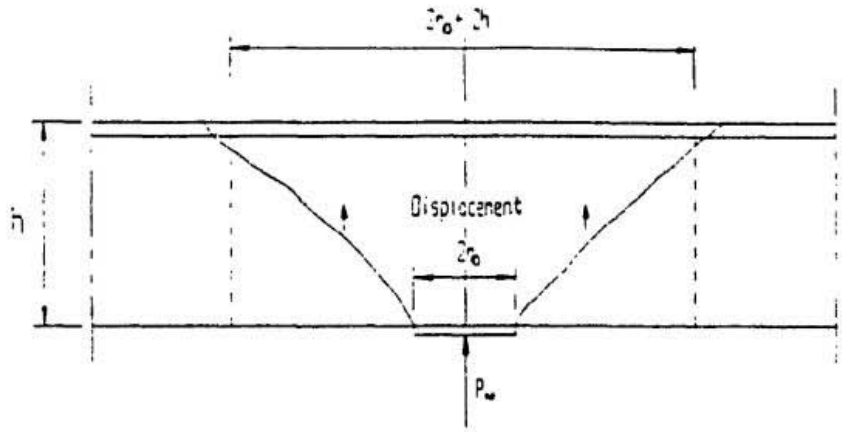

a)

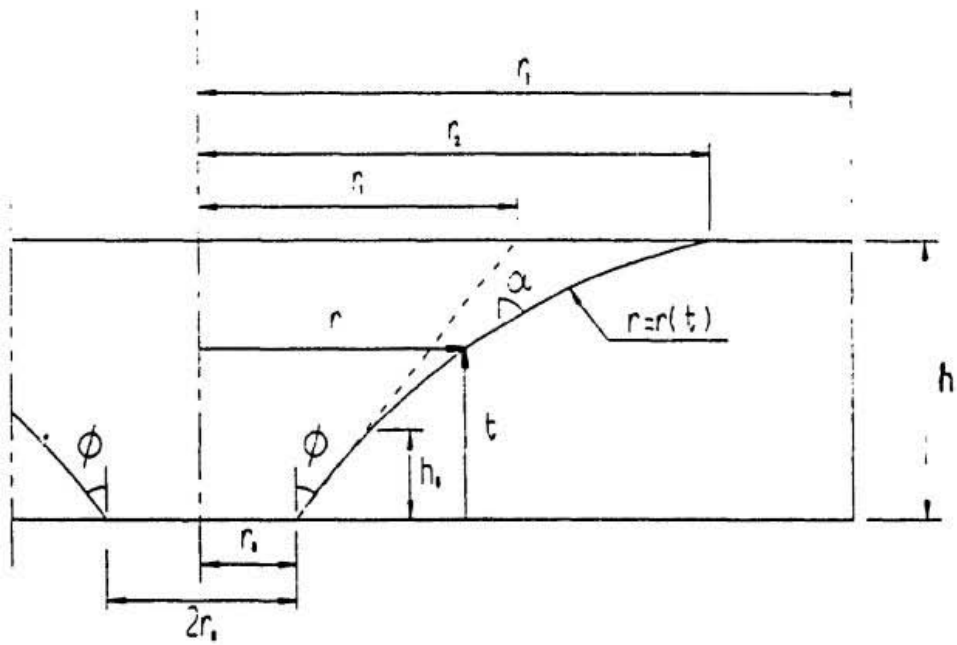

b)

Figure 2.5: Failure mechanism of Nielsen *et al.*

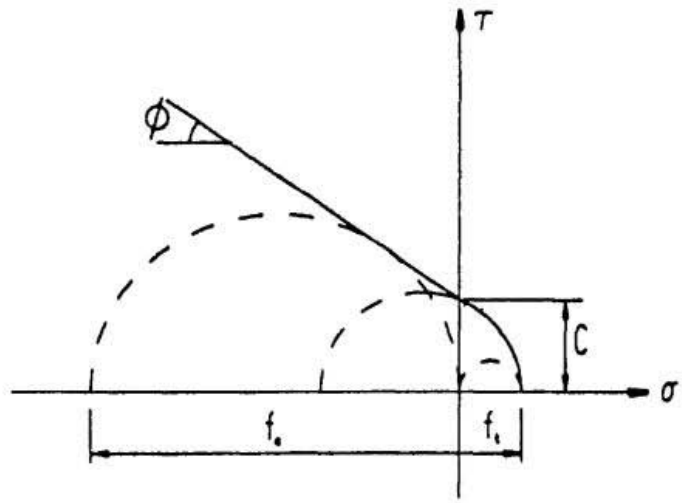

a) Modified Coulomb failure criterion

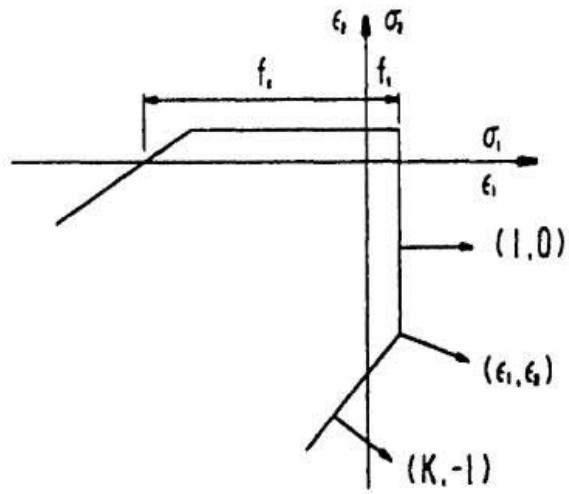

b) Yield locus in plane strain

Figure 2.6: Failure criterion and yield line locus for concrete.

a truss model (Figure 2.7) beyond the shear crack, with 45° tension and compression elements representing the behaviour of the uncracked web. Superimposed on this lattice there are additional compressions radiating from the column face below the crack.

Figure 2.7 shows the failure philosophy assumed by Andrä. He describes the failure of the concrete strut near the column face as being a restricted crushing of concrete, while, in the part of the strut far from the column face, its character is of an unrestricted splitting. It is this model which is closest in philosophy to the strut-and-tie model to be developed later in this publication.

Shehata [25], in 1985, followed by Shehata and Regan [26] in 1989, presented a model which they claimed to be an improvement over that of Kinnunen and Nylander. In that model, the effect of dowel and membrane was directly calculated from the model and the failure criterion was modified.

In 1987, Alexander and Simmonds [27] presented a truss model. The model proposed consisted of a three dimensional space truss composed of concrete compression struts and steel tension ties. The reinforcing steel and concrete compression fields were broken down into individual bar-strut units (Figure 2.8).

The truss model includes two types of compression struts: (1) those parallel to the plane of slab (anchoring struts) and (2) those at some angle α to the plane of the slab (shear struts). The model predicts only two possible failure modes for a shear strut; either the steel yields and the angle of shear strut α reaches some critical value, or the concrete fails in compression prior to yielding of steel. This implies that the traditional concepts of shear and flexure does not apply, and the two possible modes of slab failure should be classified as local connection failures as opposed to overall slab collapse.

Alexander and Simmonds stated that the evaluation of the angle α needed further

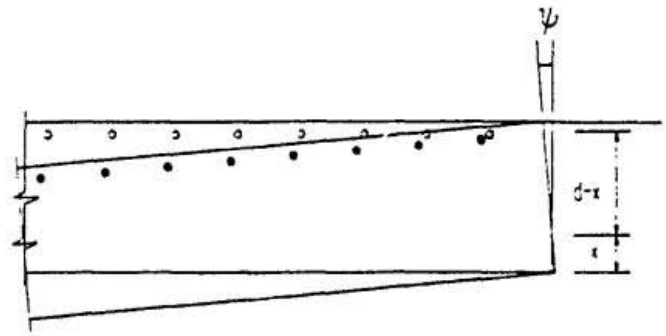

a) Rigid body rotation model adopted by Andra.

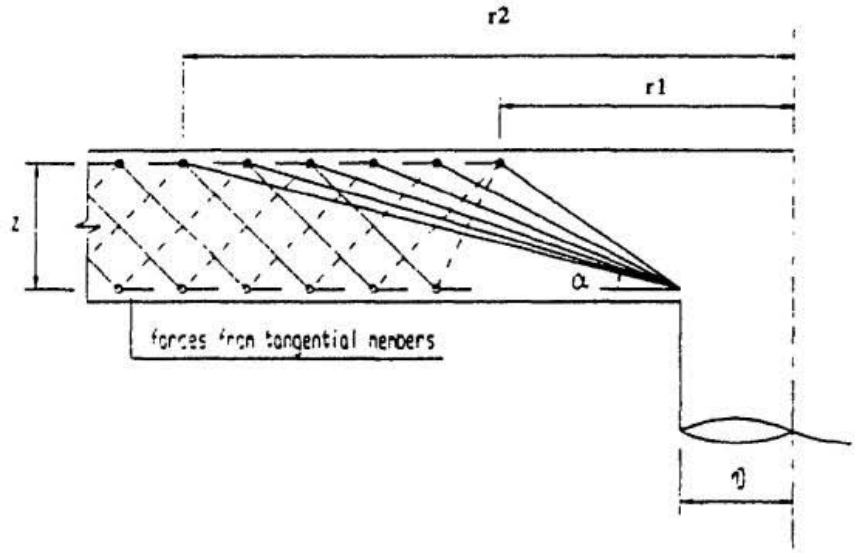

b) Andra's truss idealization of a radial segment.

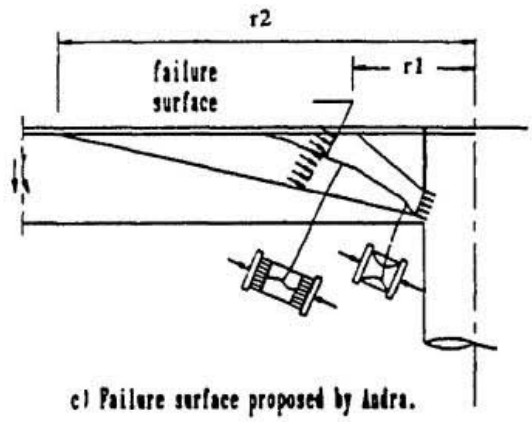

c) Failure surface proposed by Andra.

Figure 2.7: Andrã's truss model.

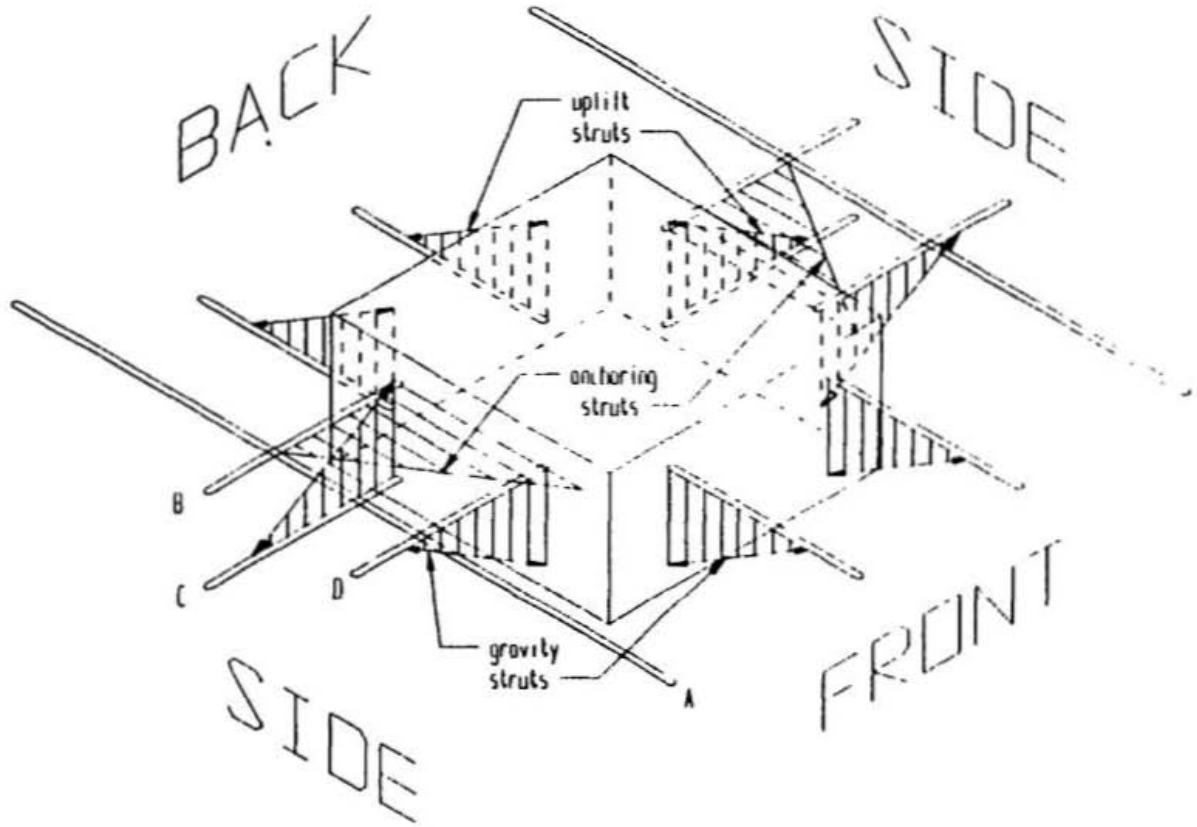

Figure 2.8: The truss model as proposed by Alexander and Simmonds.

investigation, as it was based on an empirical equation obtained from the test results.

2.1.4 North American Codes Requirements – Symmetric Punching

North American codes are based mainly on the work of Moe [1]. They are empirically based equations developed mainly from test results using slabs of relatively low compressive strengths.

The Canadian code, CAN3-A23.3-M84 [53], treats punching shear in an empirical equation found in Clause 11.10.2.

$$Vc = (1 + \frac{2}{\beta_c})0.2\lambda\phi_c\sqrt{f'_c}b_o d \qquad (2.8)$$

but not greater than

$$0.4\lambda\phi_c\sqrt{f'_c}b_o d \qquad (2.8a)$$

where

β_c = ratio of long side to short side of the concentrated load area.
b_0 = perimeter of the critical section (see Figure 2.9)
ϕ_c = resistance factor for concrete = 0.6
λ = factor to account for type of concrete
= 1.0 for normal density concrete
= 0.75 for low density concrete

The current American code, ACI 318-89 [52] has a very similar empirically based equation as the Canadian code except it is based on stress in imperial units and has a different ϕ factor. ACI clause 11.12.2.4 states

$$v_c = \phi(2 + \frac{4}{\beta_c})\sqrt{f'_c} \qquad (2.9)$$

but not greater than $4\phi\sqrt{f'_c}$ where

$$\phi = 0.85$$

2.1.5 North American Codes Requirements – Nonsymmetric Punching

The Canadian concrete code, CAN3-A23.3-M84 [53] and ACI 318-99 [52], use the empirically based linear shear stress distribution for the design. At the critical section $\frac{d}{2}$ from the face of the column of shear stress, v_f, due to a factored shear force V_f and a factored bending moment, M_f, is expressed by:

$$v_f = \frac{V_f}{b_0 d} + \frac{\gamma_v M_f c_1}{J_1} \tag{2.10}$$

For the square column of the tests (i.e., $c_1 = c_2 = c$).

$$\begin{aligned} b_0 &= 4(c+d) \\ d &= \text{effective depth} \\ \gamma_v &= 0.40 \\ c_1 &= \frac{(c+d)}{2} \\ J_1 &= \frac{d(c+d)^3}{4} + \frac{(c+d)d^3}{6} \end{aligned}$$

According to the Canadian code, no shear reinforcement is required if $v_f \leq 0.4\phi_c\sqrt{f'_c}$ (assuming $0.5\ c_1 \leq c_2 \leq 2c_1$). Shear reinforcement is required if $v_f > 0.4\phi_c\sqrt{f'_c}$. In the latter case, the following requirements have to be met:

$$v_f = v_c + v_s \tag{2.11}$$

where

$$v_c = 0.2\phi_c\sqrt{f'_c} \tag{2.12}$$

(= shear resistance of concrete)

and

$$v_s = \frac{n\phi_s A_v f_{yv}}{[s(c_2+d]} \tag{2.13}$$

(= resistance of shear reinforcement)

The ACI provisions are similar to those above, except that the resistance factors are different. According to ACI, no shear reinforcement is required if $v_f \leq 0.33\phi\sqrt{f'_c}$. If $v_f > 0.33\phi\sqrt{f'_c}$, shear reinforcement is required so that

$$v_f \leq \phi(v_c + v_s) \quad (\phi = 0.85)$$

where $v_c = 0.17\sqrt{f'_c}$.

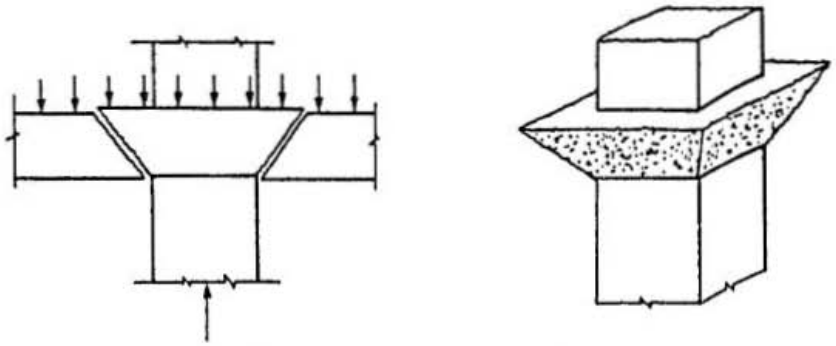

(a) Punching shear failure

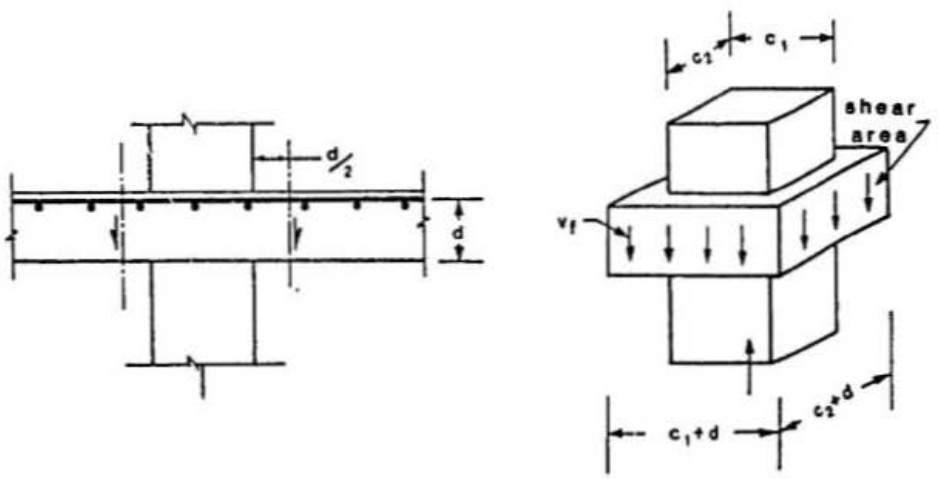

(b) Assumed critical section

Figure 2.9: Critical section for punching shear as per North American codes.

Chapter 3

Strut-and-Tie Models

3.1 Introduction

Traditional methods in the design of structural concrete members for axial load, moment, shear, and torsion have been well documented. The methods are based on the classical Bernoulli beam theory. There are, however, important regions in concrete structures where the stresses cannot be determined by these approaches. These regions are termed disturbed regions or *D*-regions. Examples of some *D*-regions in concrete structures are shown in Figure 3.1.

D-regions, if uncracked, can be designed by linear elastic stress methods, however, if they are cracked, accepted design approaches do not exist. Rules of thumb, detailing and past experience have been methods used in dealing with *D*-regions. Inelastic finite element models are capable of predicting the complex stress flows in disturbed regions, however, they are time consuming and costly for use in every-day design practices.

Considerable insight into the flow of forces can be gained by the use of strut-and-tie models. Cracked concrete carries loads through sets of compressive fields which are distributed and interconnected by tension ties. The tension ties are reinforcing bars, prestressing tendons or concrete tensile stress fields. After significant cracking has occurred, the principal compressive stress trajectories tend towards straight compressive struts. The complex internal flow of forces in disturbed regions can be modelled using concrete compressive struts, tension ties, and nodal zones which rep-

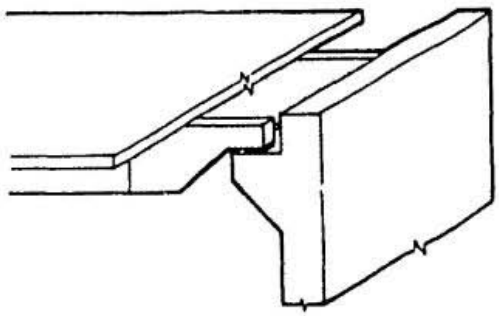

(a) Double tee with dapped end on wall corbel

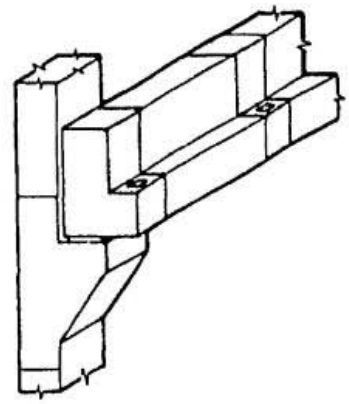

(b) Ledger beam supporting double tees

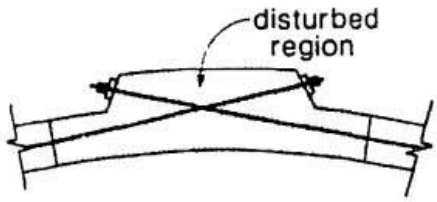

(c) Anchor buttress for post-tensioned tank

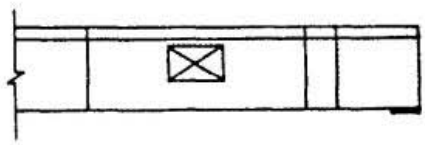

(d) Simply supported single tee with opening

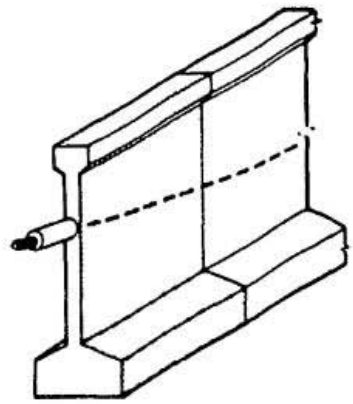

(e) Large pretensioned bridge girder post-tensioned after erection

Figure 3.1: Examples of disturbed D-regions.

resent the regions of concrete where the struts and ties meet. Various applications of strut-and-tie models are shown in Figures 3.2 and 3.3.

The use of uniaxial stressed truss members to model the stress flow in cracked reinforced concrete dates back to the turn of the century when Ritter [28] and Morsche [29] introduced the truss analogy. More recent advances have been made in the area of strut-and-tie models in Europe and in North America. Schlaich, Schaffer, and Jennewein [30] systematically expanded such models to include all parts of the structure in the hope of attaining a unified, consistent design approach for reinforced and prestressed concrete structures. Their state-of-the-art report, entitled "Toward a Consistent Design of Structural Concrete," was presented to the Comite Euro International Du Beton (CEB) in connection with the revision of the Model Code in Europe [54]. The Canadian code CAN3 A23.3 M-84 [53] includes as part of its general method of shear design, Clause 11.4, a simple design approach for disturbed regions based on the strut-and-tie model.

3.2 Components of the Strut-and-Tie Method

3.2.1 Bernoulli *B* and Disturbed *D* Regions

Reinforced concrete structures may be divided into separate design regions based on elastic strain distribution and load paths as discussed by Schlaich and Weischede [31]. The regions of a structure in which the strain distribution are linear (plane sections remain plane) are referred to as *B*-regions where *B* stands for beam or Bernoulli. For uncracked *B*-regions, stresses may be calculated from the bending and torsional moments, shears, and axial forces using section properties. For cracked *B*-regions, design methods based on the truss model may be used.

D-regions are regions having geometrical or statical discontinuities. In these re-

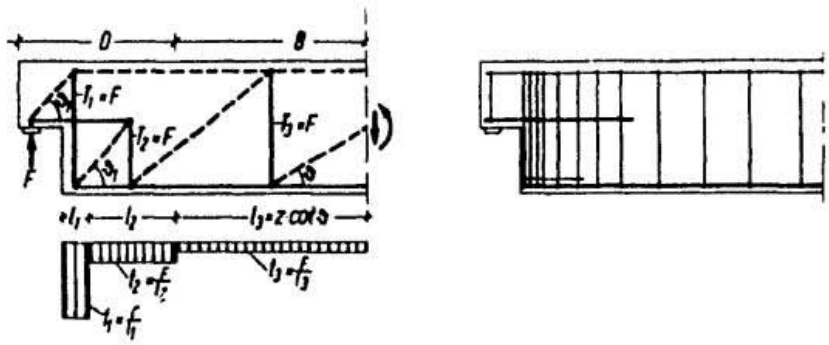

Beam with dapped end.

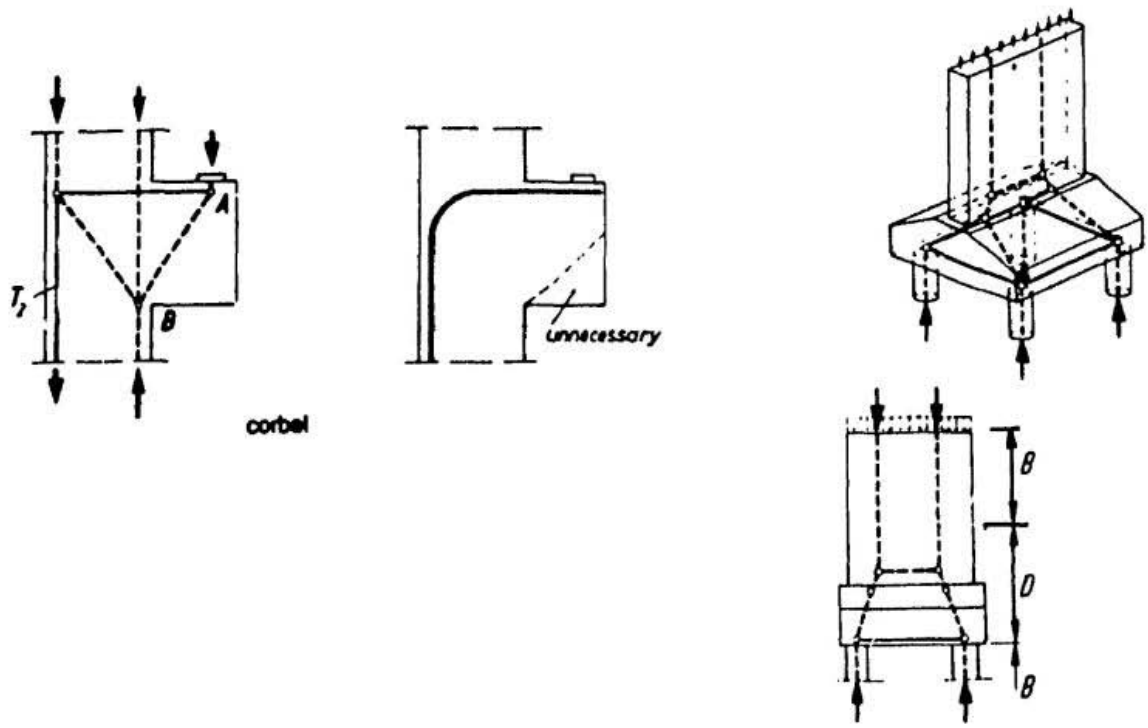

corbel

pier on a pile cap

Figure 3.2: Examples of strut-and-tie model [30].

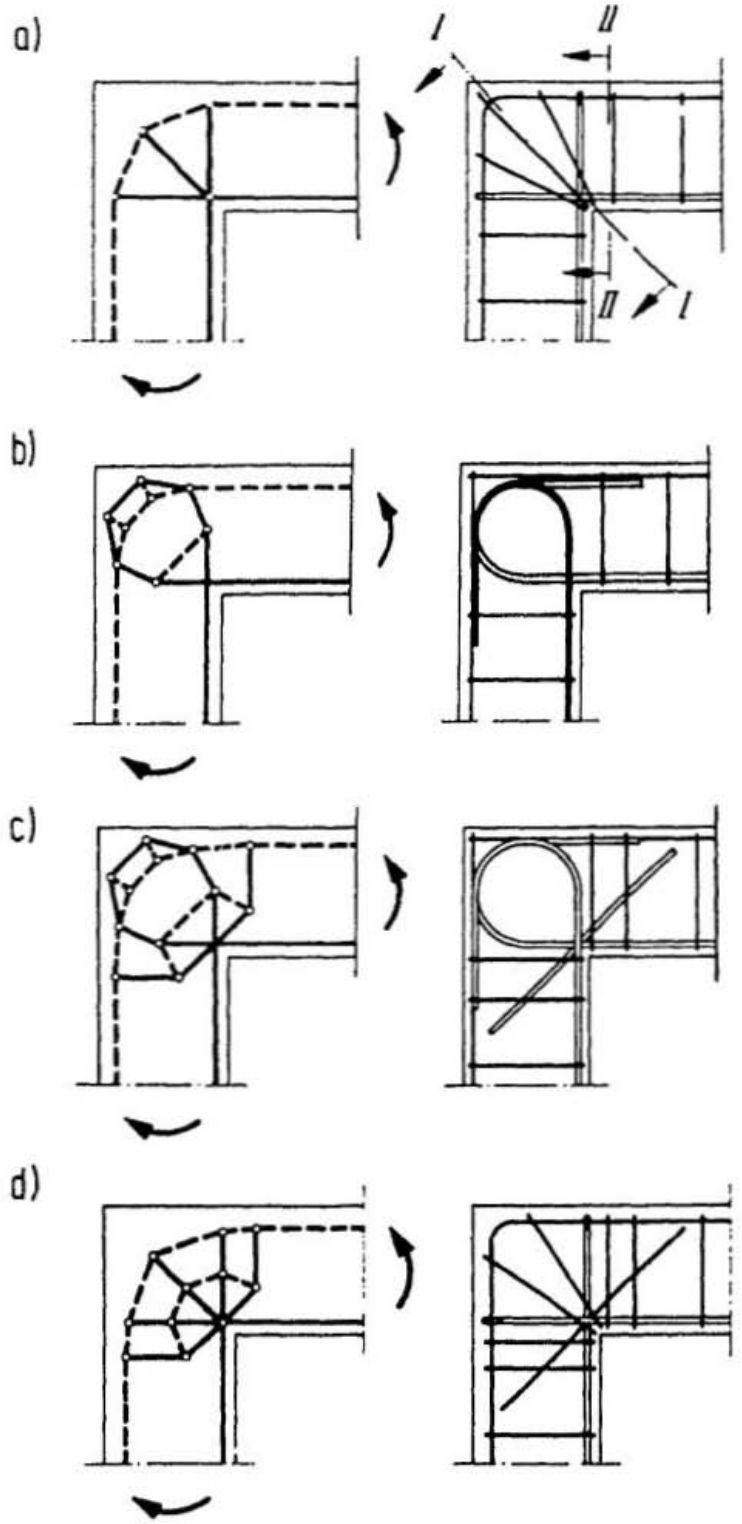

Figure 3.3: Examples of strut-and-tie model for beam/slab-column connections [30].

gions, the strain distribution is nonlinear. Examples of *D*-regions are regions near supports, opening, changes in geometry, or concentrated loads as shown in Figure 3.4. Based on St. Venant's principal, Schlaich and Weischede [31] suggest that a *D*-region may be assumed to extend approximately one depth, h, away from geometrical or statical discontinuities. Uncracked *D*-regions may be analyzed using linear elastic finite element analysis. After cracking, *D*-region behaviour is such that the traditional design procedures are typically empirically derived based on test results (corbels, deep beams). These requirements usually give guidance only concerning the provision of reinforcement, and no attempt is made to quantify stresses in the concrete. As a result, the load-carrying mechanism is unknown to the designer. A more consistent design of reinforced concrete structures is possible if strut-and-tie models are used to design these and all regions of the entire structure.

3.2.2 Tension Ties

In a strut-and-tie model, a tie force represents the total force assumed to be acting at a given location. Typically, reinforcement is provided to resist the tensile stresses, and this reinforcement is positioned such that its centroid is collinear with the assumed tension tie, see Figure 3.5. Generally, the reinforcement is assumed to be capable of providing a force equal to $A_s f_y$. In addition to providing the required amount of reinforcement at the proper location, it is also necessary to ensure that assumed forces can be developed in the reinforcement when required. For example, the tension tie in Figure 3.5 (a) provides a reaction to one face of the nodal zone and the reinforcement must have sufficient anchorage behind the nodal zone to develop this force as shown in Figure 3.5 (b).

If the tension tie represents the total force carried by an uncracked tension stress field, then the tie is located at the centroid of the stress field. Schlaich et al. [30]

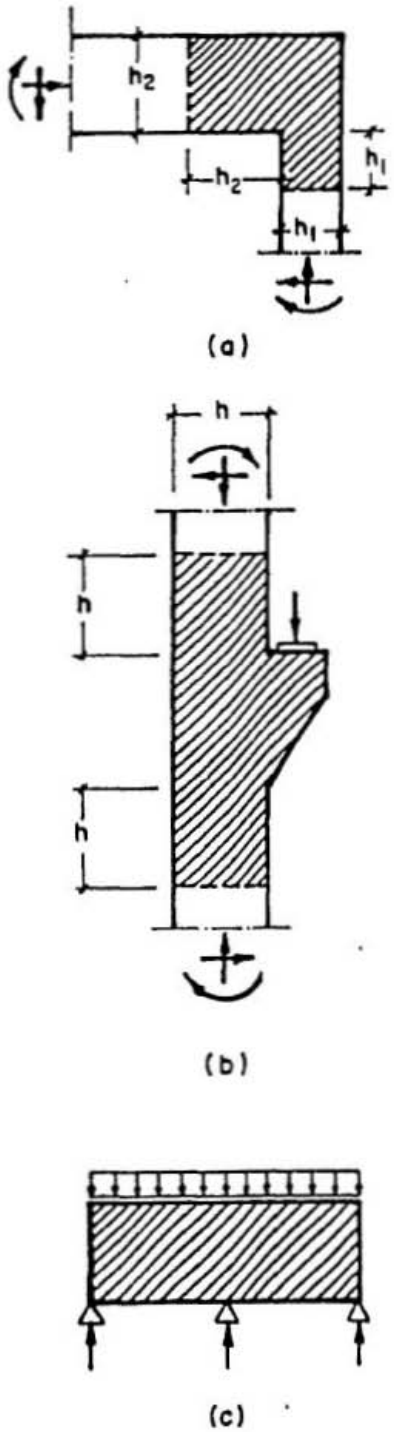

Figure 3.4: Typical *D*-regions [48].

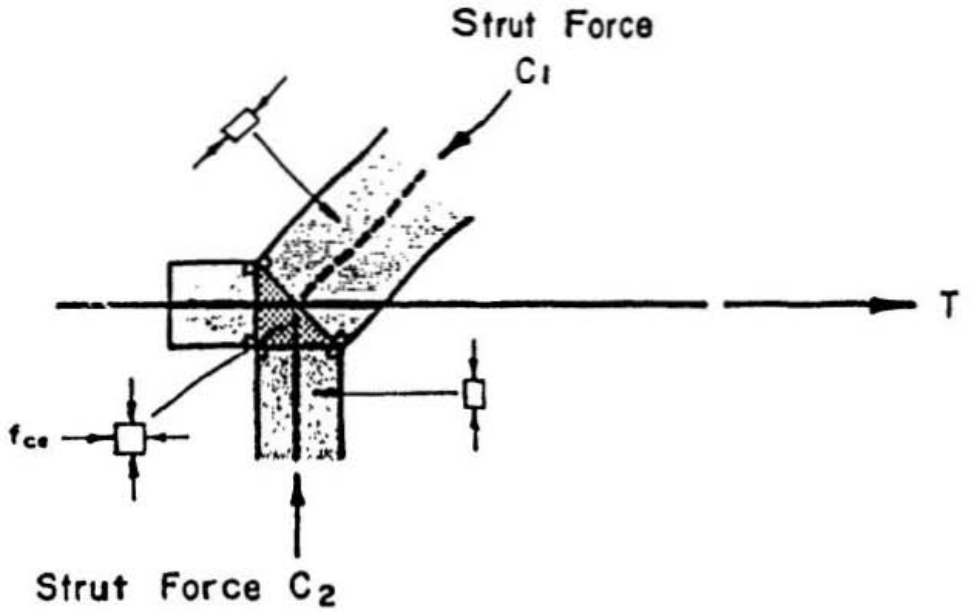

(a)

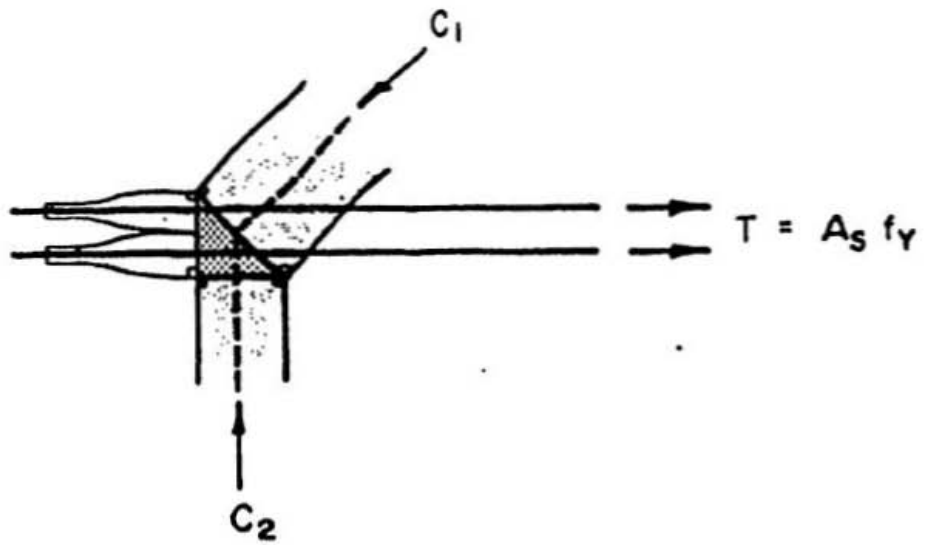

(b)

Figure 3.5: Tension tie and reinforcement [48].

suggests that until further research is available, the tensile strength of the concrete should only be used to maintain equilibrium where no progressive failure is expected. They suggest simple recommendations concerning stress redistribution and the size of the cracked failure zone relative to the area of the surrounding concrete.

3.2.3 Compressive Stress Fields

In a strut-and-tie model, compressive stress fields are used to model the way in which the compressive stresses are carried in the concrete. The three basic compressive stress fields are the strut or parallel stress field, Figure 3.6 (a), the bottle stress field, Figure 3.7 (a), and the fan, Figures 3.8-3.11.

3.2.3.1 Struts or Parallel Stress Field

The strut, as seen in Figure 3.6 (a), represents a region of concrete of width, w_s and thickness, t assumed to be stressed uniaxially to a stress equal to the effective concrete strength, f_{c2} max or f_{ce}. The maximum compressive principal stress, σ_1 is assumed to be equal to f_{ce}, and the minimum compressive principal stress σ_2 is assumed to be zero. If the strut is stressed to f_{ce} and C/t is the compressive force per unit thickness, then the width of the strut is $w_s = C/(tf_{ce})$. This stress field is largely hypothetical since in the actual structure, the stresses will generally spread out creating transverse tensile stresses. It is, however, simple to apply as shown in Figure 3.6 (b).

This figure shows a possible strut-and-tie model of a deep beam subjected to a concentrated load. This model is a simple truss with the struts carrying the compressive force C_1 and the tie providing the tension T. The shear, $P/2$, is carried by the vertical component of the compression strut. The stress of the struts is assumed to be f_{ce}. Each strut must have a vertical component T. The reaction $P/2$, strut force

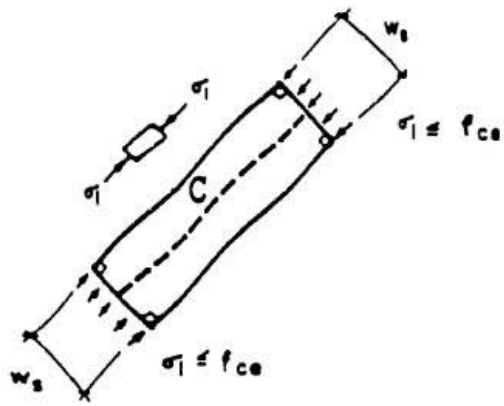

(a)

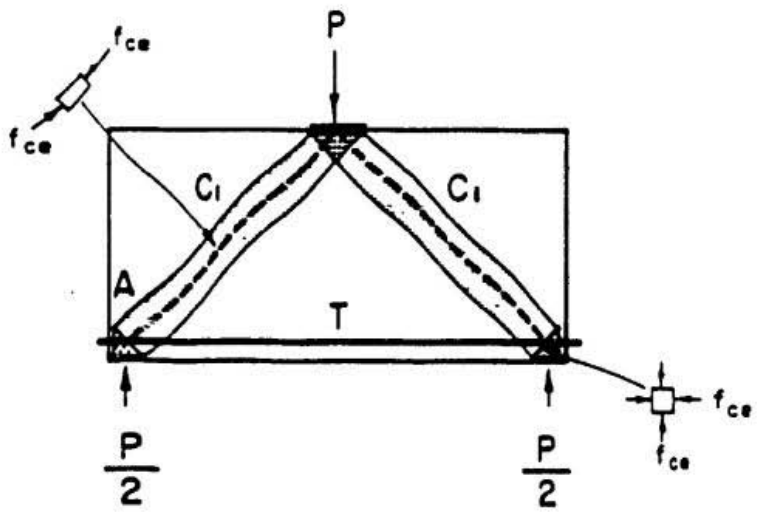

(b)

Figure 3.6: Strut or parallel stress fields and application [48].

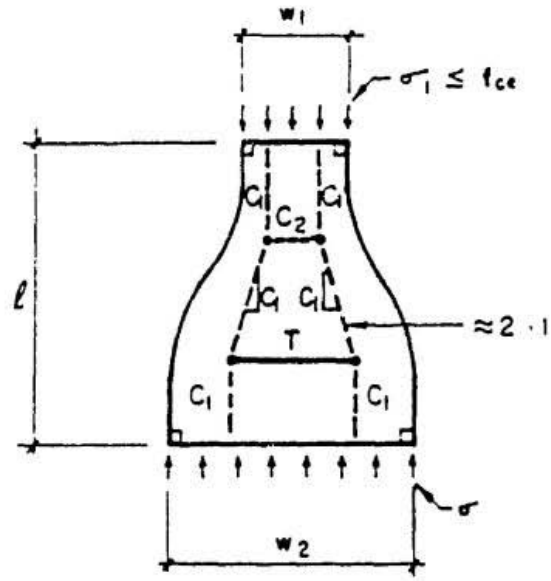

(a)

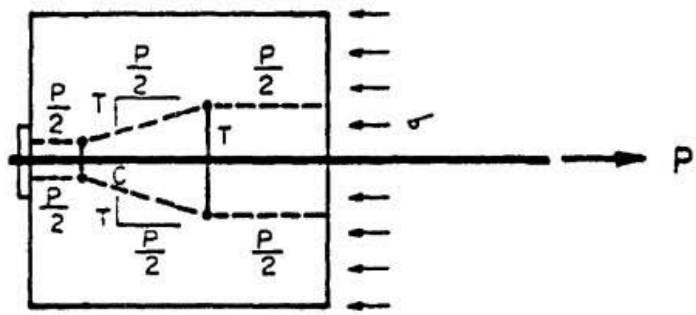

(b)

Figure 3.7: Bottle-shaped stress field and application [48].

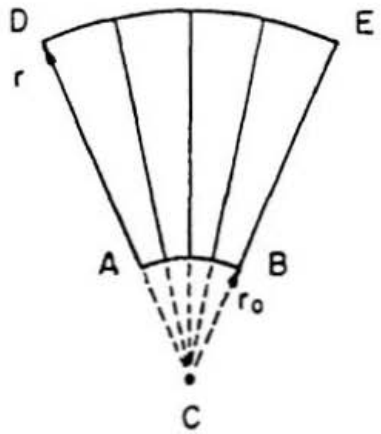

(a)

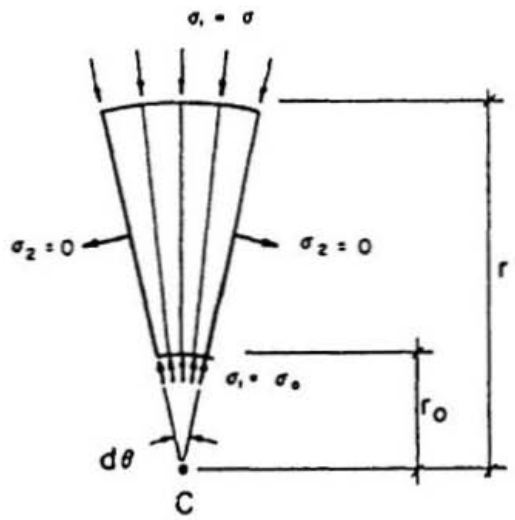

(b)

Figure 3.8: Centered fan [48].

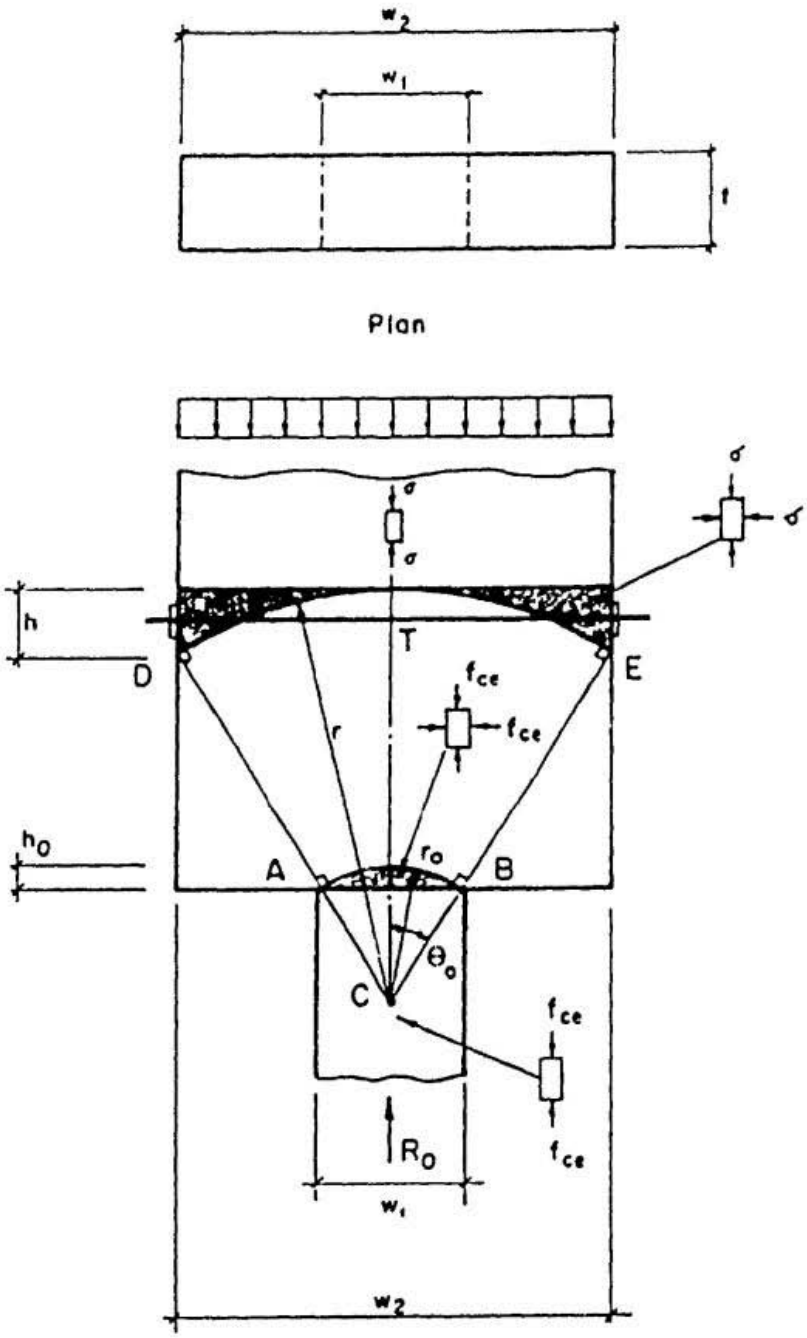

Figure 3.9: Application of centered fan stress field to spreading of a force [48].

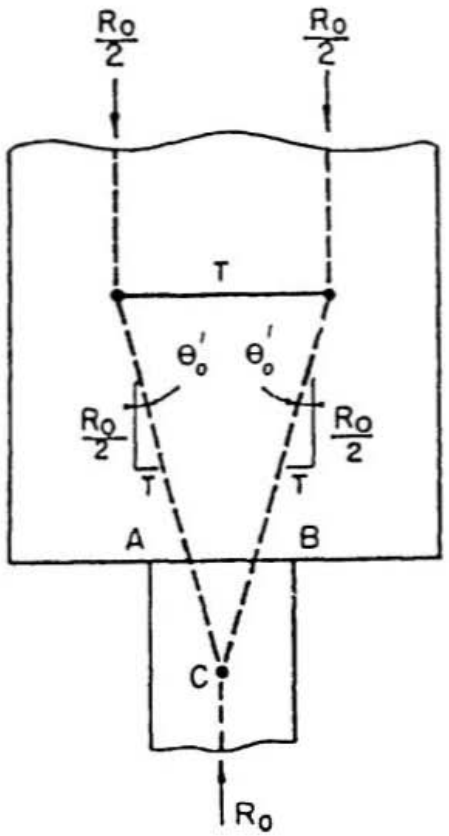

Figure 3.10: Strut-and-tie model for centered fan stress field [48].

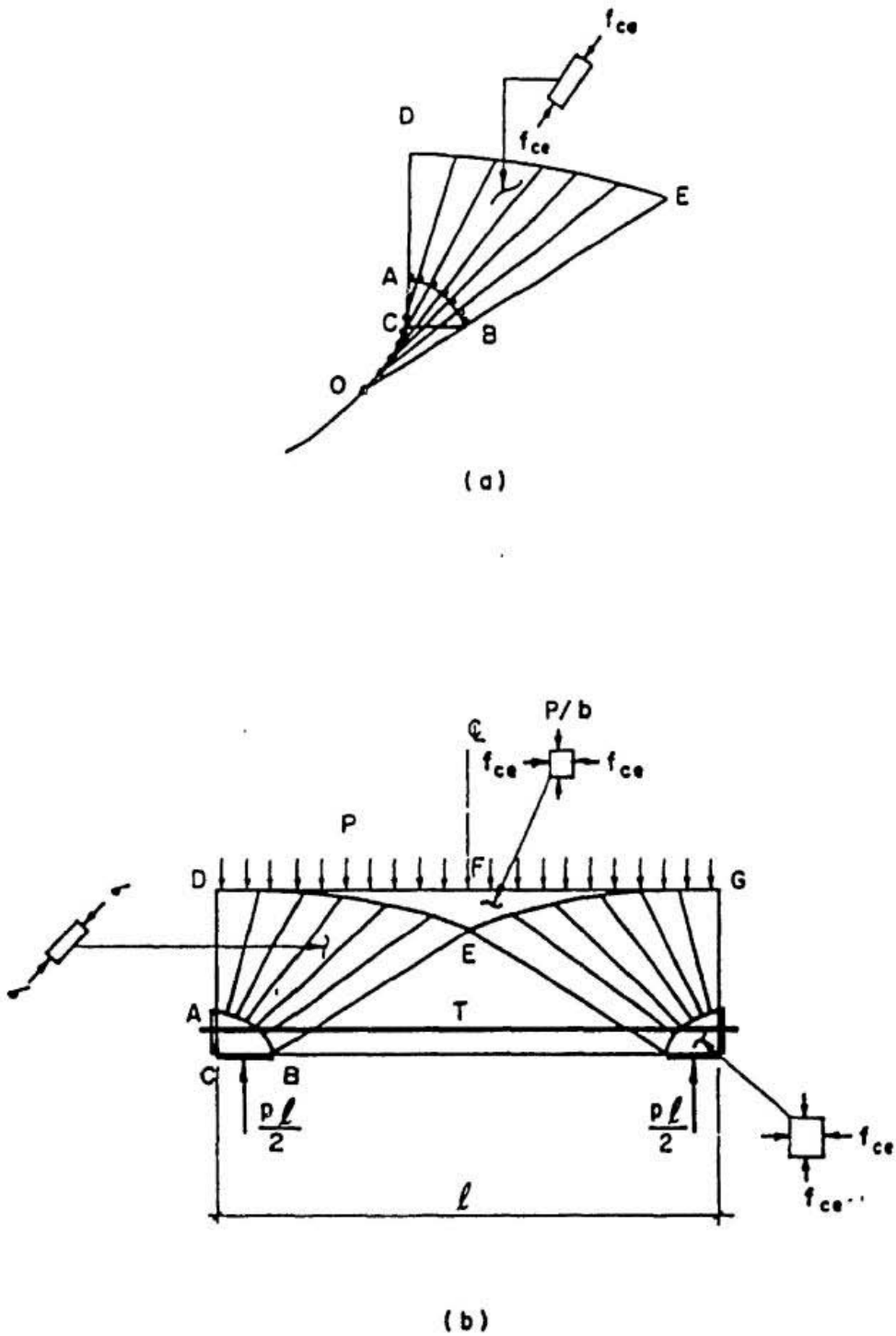

Figure 3.11: Parabolic decentered fan and application [48].

C, and tie force T must be concurrent at the node A.

For equilibrium, the nodal zone at A must have principal stresses $\sigma_1 = \sigma_2 = f_{ce}$. Nodal zones are sometimes referred to as 'hydrostatic' nodal zones although this would imply that $\sigma_1 = \sigma_2 = \sigma_3 = f_{ce}$, and in most problems, plane stress conditions are assumed ($\sigma_3 = 0$).

3.2.3.2 Bottle-Shaped Stress Fields

The bottle-shaped stress field in Figure 3.7 (a) attempts to account for the transverse tensile stress which develops when a load spreads outward from a width w_1 to a width w_2. The stress field has thickness t and length P. The load is assumed to be applied uniformly over the area $w_1 \times t$. The length ℓ measures the length over which the compressive stress trajectories spread out and then becomes parallel again. The length ℓ is generally related to w_2. This type of behaviour can be modelled with the simple strut-and-tie model shown superimposed on the stress field.

Schlaich et al. [30] give values for the load which can be safely carried by this stress field for uncracked plain concrete and for reinforced concrete. For plain concrete, the values are based on an elastic analysis considering limits on cracking ($\sigma_t < f_{ce}/15$) and on crushing of the concrete. For reinforced concrete regions, the limiting values are based on yielding of the transverse reinforcement in the tie T, and on crushing of the concrete in the neck region. This analysis was accomplished using the classic bottle-shaped strut-and-tie model shown in Figure 3.7 (a).

Figure 3.7 (b) shows an application of this strut-and-tie-model representing the spread of prestressing force P, when applied to a reinforced concrete end block and the resulting transverse tensile stresses. Typically, reinforcement is necessary to carry the 'bursting' stresses in this region.

3.2.3.3 Centered Fans

A centered fan stress field is shown in Figure 3.8 (b). The surface AB and DE have constant radii of curvature r_0 and r, respectively. The principal stress along AB is σ_0, directed radially outwards. Equilibrium of a wedge-shaped segment $d\theta$ along any of the radial fan lines requires that the principal stress along DE be given by:

$$\sigma = \frac{r_0}{r}\sigma_0 \tag{3.1}$$

The principal stress perpendicular to a radial fan line is set equal to zero. This stress field was developed to describe the transverse tensile stresses which develop due to the spreading of forces (Thurlimann et al., [32]).

A model which illustrates a centered fan is shown in Figure 3.9. The force R_0 is such that the stress in the strut below AB is f_{ce} and the nodal zone AB is stressed biaxially to f_{ce}. The stress along DE is given by Equation 3.1 as

$$\sigma = \frac{r_0}{r}f_{ce} \tag{3.2}$$

The nodal zone DE is stressed biaxially to σ. The force T represents the transverse tension required as the force R_0 spreads from width w_1 to width w_2.

The magnitude of force T may be determined from geometry and equilibrium. If the spreading angle is θ_0, then

$$r_0 = \frac{w_1}{2\sin\theta_0} \tag{3.3}$$

and the height h_0 of the node AB is given by

$$h_0 = r_0(1-\cos\theta_0) = \frac{w_1}{2\sin\theta_0}(1-\cos\theta_0) \tag{3.4}$$

From horizontal equilibrium along a vertical section through the centerline,

$$T = ht\sigma = h_0 t f_{ce} \tag{3.5}$$

If h_0 is substituted from Equation 3.4, then

$$T = \frac{w_1 t f_{ce}}{2} \frac{(1 - \cos\theta_0)}{\sin\theta_0} \tag{3.6}$$

and finally,

$$T = \frac{R_0}{2} \tan\frac{\theta_0}{2} \tag{3.7}$$

The same result may be obtained using the strut-and-tie model shown in Figure 3.10. The result suggests that reinforcement capable of resisting T given by Equation 3.7 should be provided for spreading force situations such as this.

Thurlimann, et al. [32] recommended that for most applications the spreading angle θ_0 may be taken to be 45°. Thus, $\theta_0/2 = 22.5°$ and $T = 0.21R_0$. If the strut-and-tie model shown with the bottle-shaped stress field in Figure 3.7 is used a similar result is obtained, $T = 0.25R_0$. Schlaich, et al. [30] recommend that the spreading angle be taken as 2:1.

Thurlimann, et al. [32] recommend further that the required reinforcement be distributed $1/3A_s$ in the first half of the spreading zone and $2/3A_s$ in the top half. For bottle-shaped stress fields, it is recommended that the reinforcement be distributed over the lower 0.8ℓ in Figure 3.7 (a).

3.2.3.4 Decentered Fans

If the radius of curvature of the nodal surface varies, the fan is called a decentered fan, Thurlimann, et al., [52]. In Figure 3.11 (a), line AO represents the locus of the radii to points along the nodal surface AB and along the top surface DE. It can be shown that if the principal stresses, σ_1 and σ_2, along DE are constant, then the radii must vary in such a way that DE and AB are parabolas. If the principal stresses in the nodal zone are equal ($\sigma_1 = \sigma_2$), then the fan lines will be perpendicular to the surface AB. As in the case of the centered fan, σ_1 will vary along each fan line

with radial position in the manner given by Equation 3.2, and the value of σ_2 is zero perpendicular to each fan line. Because the line DE is not perpendicular to the fan lines, there must be both a normal stress and a shear stress on the top surface of the fan.

This stress field can be used to model a uniformly loaded deep beam as shown in Figure 3.11 (b). The beam has width b and uniform load p. If the nodal zone ABC has $\sigma_1 = \sigma_2 = -f_{ce}$ then $\sigma_2 = -p/b$. For horizontal equilibrium, the height of the nodal zone AC must be equal to the height of the nodal zone EF.

3.2.4 Nodal Regions

The regions where compressive struts and tension ties meet are called nodal zones. The nodal zone is an idealized representation of the way in which the compressive stress field and tension ties intersect.

Nodal zones may be classified according to the type and number of forces which intersect there. When three forces meet, equilibrium requires that the forces be concurrent. When three compressive forces meet, the nodal zone is called a CCC nodal zone as shown in Figure 3.12 (a). Typically, the magnitude of the stress in each in each of the struts is taken to be equal to f_{ce}. This means that the line of action of each force will be perpendicular to one side of the nodal zone and that the widths of the sides are in the same proportion as the magnitudes of the forces. The state of stress of the nodal zone will be $\sigma_1 = \sigma_2 = -f_{ce}$. The force triangle will be similar to the triangle ABC of the nodal zone. The nodal zone, ABC of Figure 3.12 (b), is an example of a triangular CCC nodal zone with equal stresses. The load P is applied through a bearing plate of width greater than or equal to the width AB such that the stress along AB is $-f_{ce}$. Similarly, the widths of the struts are such that the principal stresses along AC and BC are also $-f_{ce}$.

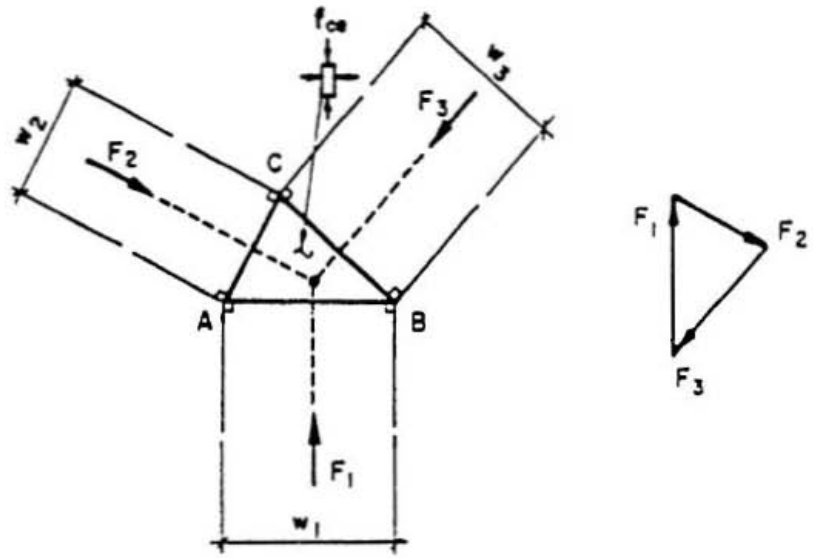

(a)

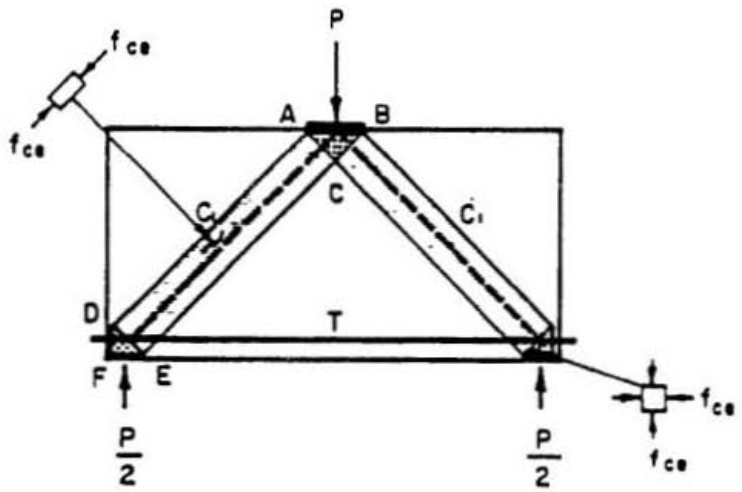

(b)

Figure 3.12: Triangular three compressive forces nodal zone [48].

A *CCC* nodal zone with curved surfaces is shown in Figure 3.13 (a). An application of this nodal zone is found in the uniformly loaded deep beam in Figure 3.13 (b). In this nodal zone, the principal stresses are $\sigma_1 = -q/b$ and $\sigma_2 = -f_{ce}$ where q is the applied load and b is the width of the beam. Principal stresses along *AC* and *BC* vary according to the geometry of the fan. It is seen that the fan lines are not perpendicular to the nodal surface. By considering horizontal equilibrium, it can be shown that the width of the nodal zone at *C* must be equal to the height of the nodal zone at *DF*.

In a *CCT* nodal zone, two compressive forces meet a tension tie. A *CCT* nodal zone may be triangular as shown in Figure 3.14 (a) or it may have curved surfaces, see Figure 3.14 (b). If the stresses in the struts are equal to f_{ce}, then the nodal zone has $\sigma_1 = \sigma_2 = -f_{ce}$. The line of action of each force and each fan line is perpendicular to the surface of the nodal zone.

CCT zones are often idealized as having an anchor plate which allows the tie to develop outside the nodal zone so that the nodal zone behaves like a *CCC* nodal zone through which a tension tie passes. It is because of this strain discontinuity that the recommended effective concrete strength for *CCT* nodes is often reduced (Schlaich, et al. [30]; CAN3 A23.3-M84 [53]). The nodal zone *DEF* in Figure 3.12 (b) and in Figure 3.13 (b) is a typical example of a *CCT* node. Typically, anchor plates are not used, and the reinforcement represented by the tension tie must develop by bond anchorage and/or hook anchorage. The force in a reinforcing bar is transferred to surrounding concrete by compressive stresses. It is because these stresses change direction that transverse tensile splitting stresses develop. In regions where these transverse stresses are limited or prevented, straight bar anchorage or bond is enhanced. In a *CCT* region at a support, for example, the reactive force and the strut act to prevent the formation of the transverse tensile stresses thereby improv-

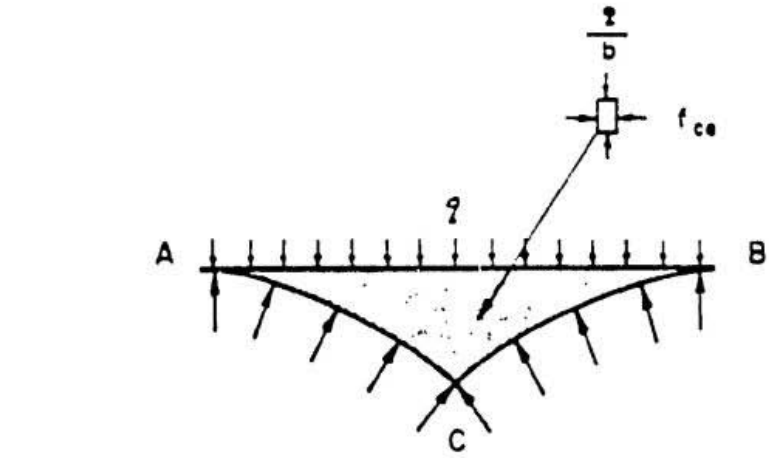

(a)

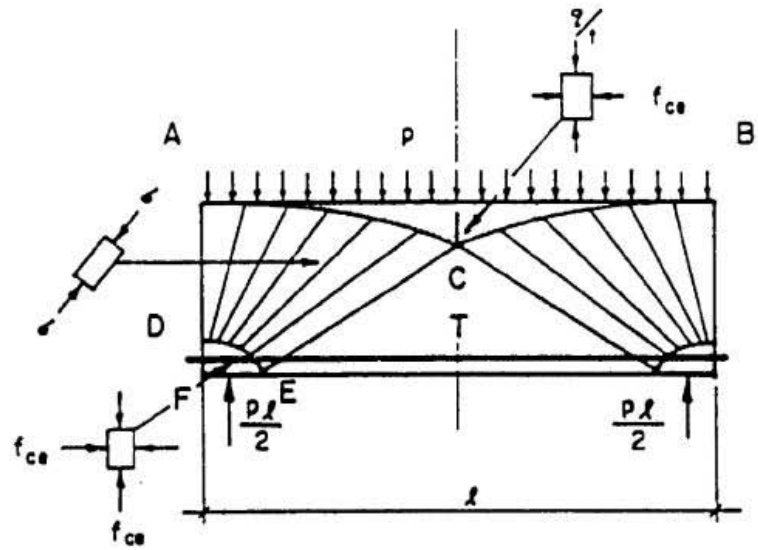

(b)

Figure 3.13: Curved three compressive force nodal zone [48.]

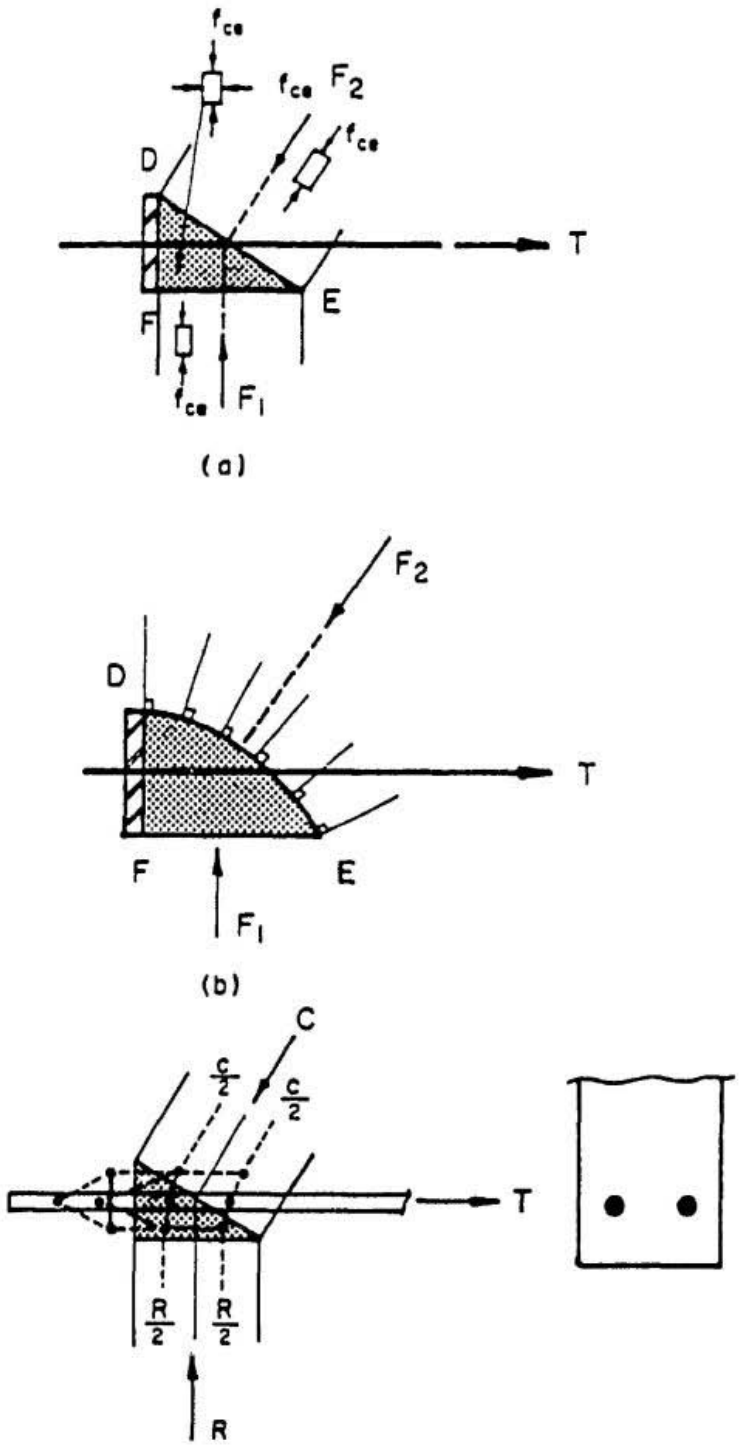

Figure 3.14: Compression-compression, tension force nodal zone [48].

ing the bond. However, outside the region of the joint, sufficient anchorage must be provided for the force remaining in the bar. Before a CCT node can be completed, the anchorage of the tension tie must be considered.

Other three-force nodal zones are the CTT and TTT nodal zones. A typical CTT nodal zone occurs where stirrups, longitudinal reinforcement, and a compressive stress field meet, as in the case of beams with shear reinforcement.

3.3 General Modelling Procedures

If the structure consists of a single D-region, the strut-and-tie forces are determined directly from the applied loads and statically determinate reactions. In order to develop the strut-and-tie model for structures which are statically indeterminate or are composed of D- and B-regions, the reactions must be determined by structural analysis. Generally, a linear elastic analysis is suitable although in extreme cases where the structure is heavily cracked and forming plastic hinges, a nonlinear analysis would be more acceptable. Suggestions regarding the structural analysis for the ultimate and serviceability limit states are given by Schlaich, et al. [30].

An elastic analysis has the advantage of being simple and readily available, and it is suitable for checking serviceability. The elastic analysis could be any of the standard techniques although the stress distribution obtained from a linear elastic finite-element analysis is very useful when developing the strut-and-tie model.

In developing the strut-and-tie model, it is helpful to realize that most B-regions can be designed using the truss model (CEB-FIP Model Code [54]) or truss model based on the compression field theory (CAN3 A23.3-M84 [53]). The results of this provide the internal forces at the junctions with any adjacent D-regions. Once the forces at the boundary of the D-region are known, it is possible to develop the load path within the region. The majority of D-regions contain a very clear load path and

involve standard models.

Structures are generally insensitive to small deviations in the position of the reinforcement, and to some extent, will carry the load in a manner consistent with how they are reinforced. It has been suggested that the strut-and-tie model with the least volume and shortest length of ties is desired. Schlaich and Weischeide [31], Schlaich, et al. [30]. This assumes that the loads try to follow a load path which minimizes forces and deformations and since the ties are much more deformable than the concrete struts which have much larger volume and lower strains, the model with the least and shortest ties more closely models the actual behaviour.

It has been suggested that the struts and ties should be oriented following the elastic stress trajectories, Schlaich et al. [30]. This should limit the amount of redistribution required after cracking. They state that this approach will provide a conservative ultimate strength design, and they recognize the potential benefit in being able to use the same elastic analysis for serviceability design. If the elastic stress distribution is not known, then the strut-and-tie model can be based on an estimate of the load path.

In all cases, it is important to consider the ductility of the model. It is necessary to ensure that the rotation capacity of the structure is not exceeded at any location before the assumed state of stress exists in the remainder of the structure. In highly stressed regions, this should be fulfilled if the struts and ties are oriented with the elastic stress trajectories and the internal forces were determined from an elastic analysis since these forces were maximum prior to redistribution. In regions that are relatively low stressed, the struts and ties may deviate considerably from the elastic stress distribution allowing the reinforcement to be arranged according to practical considerations. Such is the case in a typical *B*-region where stirrups are provided orthogonally to the principal reinforcement rather than along the principal tensile

stress trajectories.

In some cases, it may be necessary to use a nonlinear finite element analysis. This can be difficult for design since the reinforcement and perhaps even the geometry are not known at the start. For these special cases, the recommended technique is to first use an elastic finite element analysis to develop a strut-and-tie model to provide a check of the geometry and proportions the reinforcement for ultimate strength. Then, if desired, a nonlinear finite element analysis can be used to check the completed design. It is recommended in all cases that a strut-and-tie model be used to verify the results of a nonlinear finite element analysis. The greater the degree of sophistication of the structure the greater the need for a simple design check.

3.4 Canadian Code Requirements

This section summarizes the strut-and-tie model approach for the design of disturbed *D*-regions. The provisions of the Canadian concrete code, CAN3 A23.3-M84 [53], have been used. The Canadian code uses load factors of 1.25 and 1.50 for dead load and live load, respectively. Material resistance factors of $\phi_c = 0.6$ for concrete, $\phi_s = 0.85$ for reinforcing bars and $\phi_p = 0.90$ for prestressing tendons are used.

In designing a disturbed region, the first step is to visualize the flow of forces in the region and locate the nodal zones. The nodal zones must be made large enough to ensure that the stresses satisfy the code limits. The Canadian code requires that the concrete compressive stresses in the nodal zone do not exceed $0.85\phi_c f'_c$ in nodal zones bounded by compressive struts, and $0.75\phi_c f'_c$ in nodal zones anchoring one tension tie, and $0.6\phi_c f'_c$ in nodal zones anchoring tension ties in more than one direction, refer to Figure 3.15.

The next step is the idealization of the truss model geometry. The nodes of the truss are located at the points of intersection of the forces meeting at the nodal zones. The forces in the truss model are determined by statics.

After determining the forces in the truss members from statics, the required area of tension tie reinforcement is chosen. The tension tie reinforcement must be anchored so that it can transfer the required tension to the nodal zone of the truss. Additionally, the tension tie reinforcement must be distributed over an effective concrete area equal to the tension tie force divided by the nodal zone stress limit, see Figure 3.15 again.

The concrete compressive stress, f_{c2}, in the struts must not exceed the crushing strength of cracked concrete, f_{c2} max, which is given by:

$$f_{c2}\,\max = \frac{\lambda\phi_c f'_c}{0.8 + 170\epsilon_1} \leq \phi_c f'_c \tag{3.8}$$

The maximum compressive stress the strut can carry decreases as the principal tensile

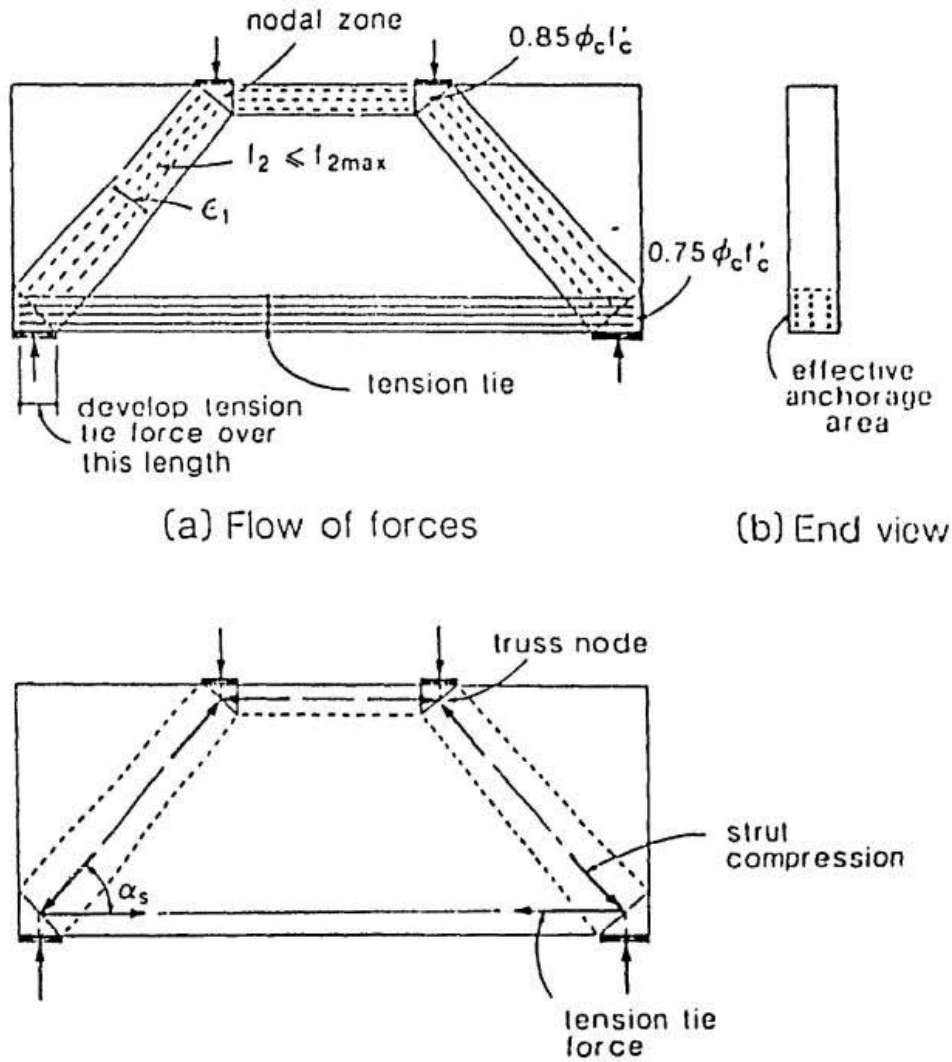

Figure 3.15: Strut-and-tie truss model for a deep beam.

strain ϵ_1 increases. The principal tensile strain ϵ_1 is determined from strain compatibility in regions where a tension tie crosses a compressive strut. From Mohr's circle for strain, if ϵ_x is replaced by the strain ϵ_s in the tension tie, if θ is replaced by the angle α_s between the tension tie and the strut, and if it is assumed that the compressive strain in the strut is 0.002, then

$$\epsilon_1 = \epsilon_s + \frac{\epsilon_s + 0.002}{\tan^2 \alpha_s} \tag{3.9}$$

The strain in the tension tie may be assumed to be fy/E_s. The basis of this approach is from work carried out in Canada by Vecchio and Collins [50] and Collins and Mitchell [51]. This work found that the principal compressive concrete stress, f_{c2}, is not only a function of the principal compressive strain, ϵ_2, but also depends on the principal tensile strain, ϵ_1. As ϵ_1 increases, f_{c2} decreases – an effect that has been termed "concrete strain softening." The compressive stress-strain relationship from cracked concrete can be expressed as

$$f_{c2} = \beta f'_c [2\left(\frac{\epsilon_2}{\epsilon'_c}\right) - \left(\frac{\epsilon_2}{\epsilon'_c}\right)^2] \tag{3.10}$$

where

$$\beta = \frac{1}{0.8 + 0.34(\epsilon_1/\epsilon'_c)} \leq 1.0.$$

The stress limit, f_{c2} max in Equation 3.8 can be derived by setting ϵ'_c and ϵ_2 equal to 0.002. Once the compression strut and tension ties are checked, the designer should provide uniformly distributed well-anchored reinforcing bars in both the vertical and horizontal directions. These bars control cracking and improve ductility.

Chapter 4

Proposed Strut-and-Tie Model for Punching Shear of Concrete Slabs

4.1 Symmetric Punching Shear of Concrete Slabs

4.1.1 Introduction

Figure 4.1 shows the general punching shear behaviour of a uniformly loaded slab supported by a circular column. The applied uniform load can be replaced by an equivalent point load. The inclined shear crack which develops from the top surface at an angle, θ, and forming the critical section is shown. The top layer of flexural reinforcement which plays an important role in the strut-and-tie model is also shown in this figure. Although it is known that flexural reinforcement plays a part in determining the punching shear strength of a slab, most empirical procedures and the current North American design codes neglect it entirely. In general, the inclined shear crack forms at a load level of less than 70 percent of the ultimate punching load [33]. These cracks form at the critical section and completely surround the column. The slab at this level can be unloaded and reloaded without any decrease in the ultimate punching capacity. This compressive zone which extends a distance of $h - y$ from the top face of the slab will be termed as the crack-zone. Cracking in this zone is dependent on the diagonal tensile strength of the concrete. The second zone which extends at an angle of $\frac{\theta}{2}$ is made up of a compressive zone extending to the face of the column

at a height of y. This zone is where the ultimate punching shear capacity of the slab is governed. Punching of the slab occurs when the concrete in this zone fails by a high concrete compression stress. This second zone will be termed the ultimate failure zone. For normal strength concrete, the angle of inclination θ has experimentally determined to be between 26 and 30 degrees whereas for high strength concrete the angle varies between 32 and 38 degrees as determined through experimental testing by Hussein [39] at Memorial University of Newfoundland.

4.1.2 Stress Fields – Strut-and-Tie Model

Figure 4.2 shows the stress fields in the slab due to symmetric punching shear. The crack zone is made up of a bottle-shaped compression field in which the tensile strength of the concrete perpendicular to this field controls cracking. The ultimate failure zone is a parallel shaped compression field. From these stress fields a refined strut-and-tie model is developed as indicated in Figure 4.3.

The ultimate failure zone is the important zone relative to ultimate punching shear capacity. Punching will occur in this region due to high radial stress leading to a compressive failure in the concrete.

The zones in these figures are shown in two-dimensional for simplicity, however, they are actually three-dimensional "cone shaped" fields located around the perimeter of the column.

4.1.3 Shear Cracking – The Crack Zone

A refined strut-and-tie model can be developed in the upper zone of the proposed model (Figure 4.3). Two compression struts radiate at dispersion angles of approximately 2:1 (as proposed by Schlaich et al. [30]) from the angle of inclination, θ.

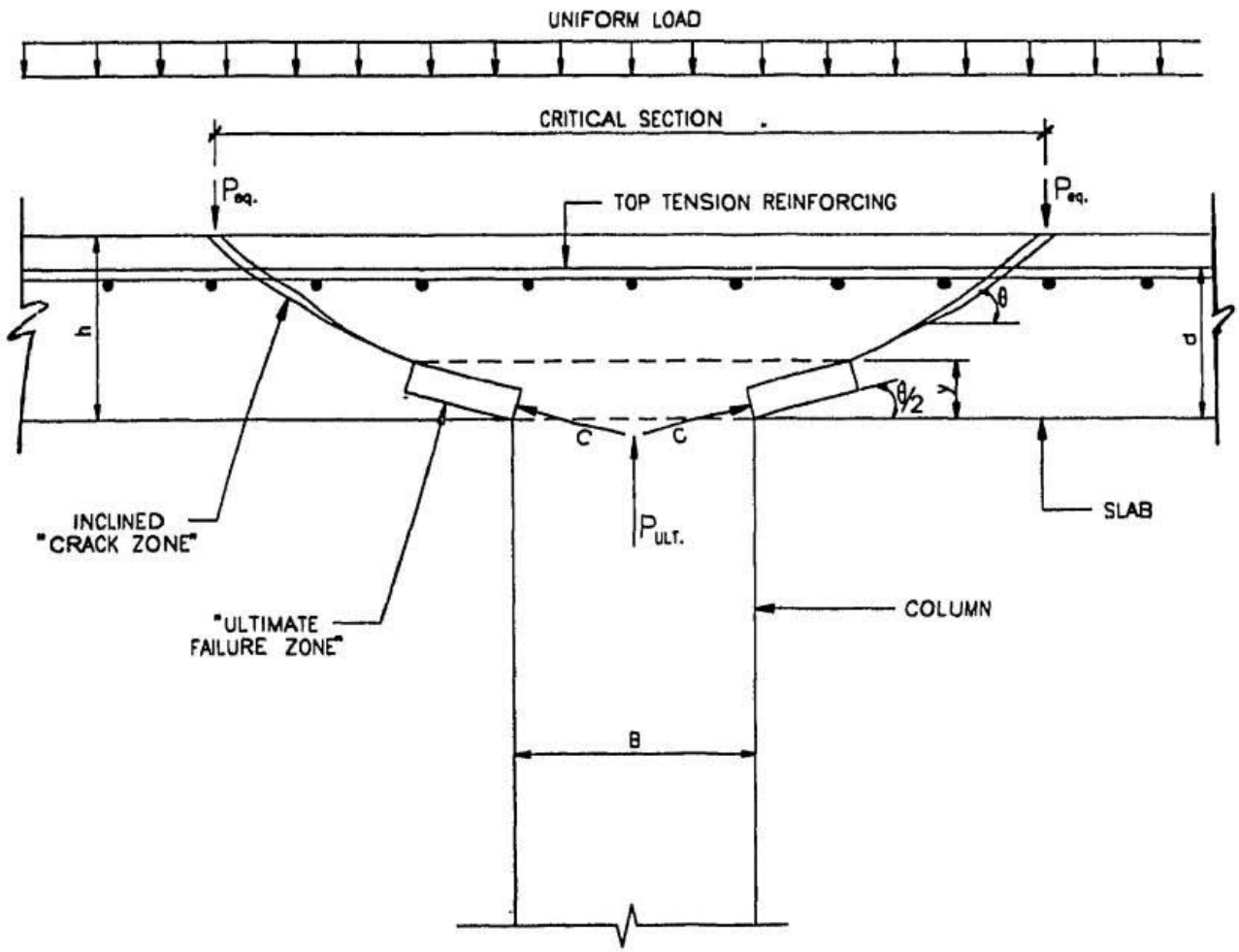

Figure 4.1: Punching shear behaviour of concrete slab.

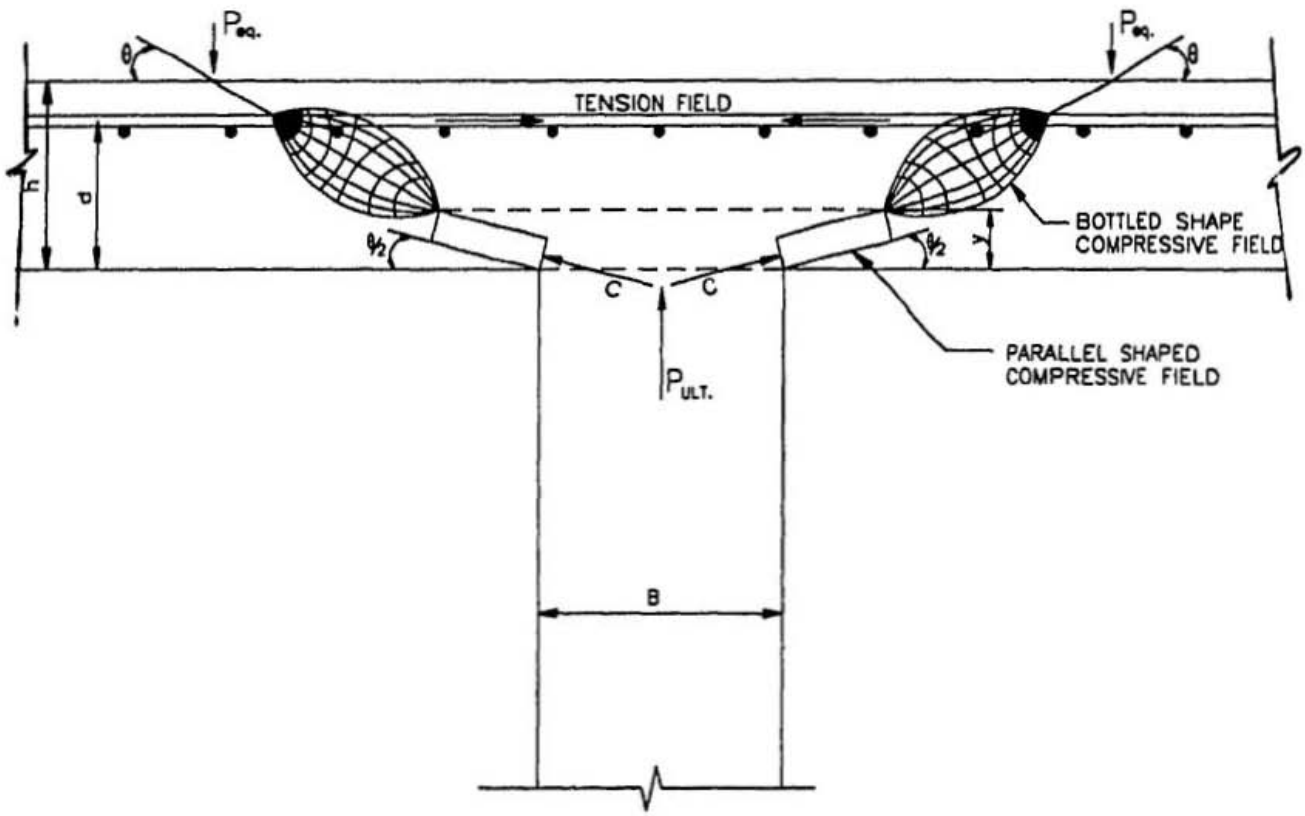

Figure 4.2: Stress fields due to symmetric punching.

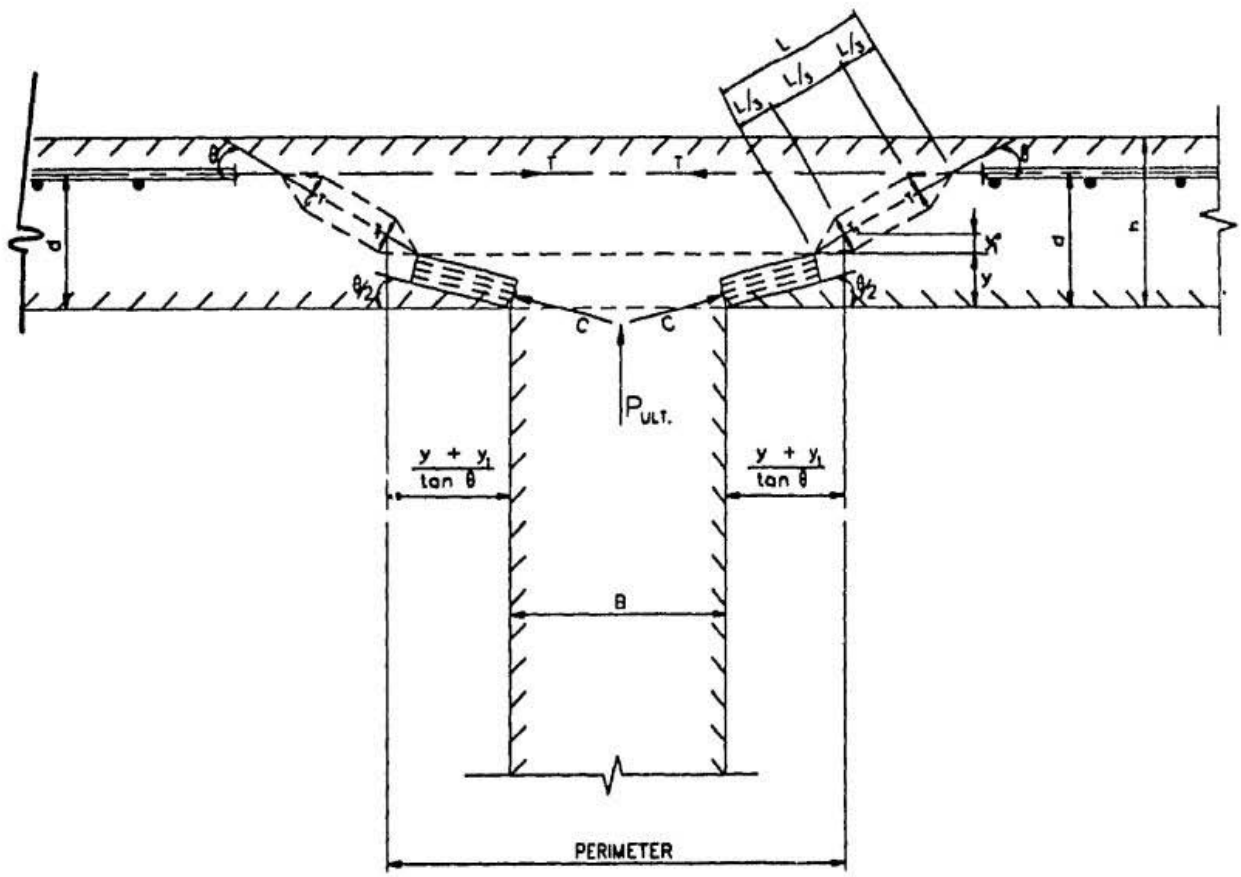

Figure 4.3: Refined strut-and-tie model for symmetric punching of concrete slab.

The compression forces are held together by two perpendicular tensile forces in the concrete. Cracking occurs when the stress in these tensile zones equals or exceeds the tensile strength of the concrete, f_t. The tensile strength of the concrete as determined by experimental testing conducted by Marzouk and Chen [49] at Memorial University of Newfoundland can be taken as

$$f_t = 0.05 f'_c \qquad \text{high strength concrete} \tag{4.1}$$

and using CAN3 A23.3.M84 [53] for normal strength concrete

$$f_t = 0.5\sqrt{f'_c}.$$

The punching shear cracks which develop in the crack form at a load level less than the ultimate punching shear load. The slab remains stable and may be loaded and reloaded after these cracks form [33]. The punching shear crack load can be established by equating and solving the inclined truss shown and comparing the tension force to f_t of the concrete.

It is assumed the inclined length of the crack zone is L, as shown in Figure 4.3, and that cracking will occur first in the lower tension tie due to its lower perimeter relation with the column. The contributing width to the lower tie can be taken as $L/3$ and the perimeter of the critical section with respect to the column as $\pi\left(B + 2\left(\frac{(y+y_1)}{\tan\theta}\right)\right)$. The cracking load can then be approximated from geometry by the following equation.

$$T = \frac{f_t \cdot L}{3} \cdot \pi\left(B + 2\frac{(y+y_1)}{\tan\theta}\right) \tag{4.2}$$

where

$y =$ depth of flexural compression zone in slab

$$L = \frac{d - y}{\sin\theta}$$

$$y_1 = \frac{L \sin\theta}{3}$$

$B =$ diameter of column. (A square column can be replaced in the equation by an equivalent circular column with the same perimeter, i.e., $B = \frac{4c}{\pi}$.)

The spreadsheet computer program "PUNCH." developed by the author, includes the above equation, see Appendix A.

Although ultimate punching shear failure of the slab is not dependent on the crack zone, this zone is important in that that presence of cracking in this zone around this periphery of the column may be a warning sign the applied loads are nearing the ultimate punching shear level. In many structures, such as offshore structures, crack control is an important serviceability limit state. The presence of punching shear cracks in these applications are to be avoided and knowledge of the cracking mechanism behaviour is required.

4.1.4 Punching Failure Mechanism – Ultimate Failure Zone

In flat plate concrete slabs, inclined shear cracks usually form at a load level of less than 70 percent of the ultimate load. These cracks can completely surround the column, the slab is nevertheless stable, and can be unloaded and reloaded without any decrease of the ultimate load [33]. It is therefore evident that the ultimate failure mechanism is not normally a pure "shear failure" governed by the diagonal tensile strength of the concrete. Punching shear failure occurs when the concrete in compression in a parallel stress field near the column fails by a high radial compressive stress. Pult denotes the corresponding ultimate punching shear capacity failure mech-

anism. The basis of this approach has been successfully developed by the rational model developed by Kinnunen and Nylander [13] and Andrä's truss model [24] modified to conform to the strut-and-tie design requirements of the present Canadian concrete code. This approach is used as a basis in the proposed strut-and-tie model to determine the ultimate punching capacity of a slab under symmetric loading.

4.1.4.1 High Radial Compression Stress Failure Mechanism

The parallel stress compression zone in the vicinity of a circular column, is shown in Figure 4.4. The column force Pult is transferred to the slab via inclined radial forces that must pass under the root of the shear crack. The inclination of the crack is assumed to be between 26 degrees and 32 degrees for normal strength concrete and between 32 and 38 for high strength concrete [39]. The crack is assumed to have propagated down to the neutral axis at flexure in the radial direction.

The radial compressed concrete strut is assumed to form an imaginary conical shell-strut with constant thickness, at an angle inclination that is $\frac{\theta}{2}$. Punching shear failure is assumed to occur when the stress in the conical shell-strut reaches the value of the crushing strength of cracked concrete, f_{c2} max, given by Equation 3.8.

The refined strut-and-tie model of Figure 4.3 shows the complete force fields developed due to symmetric punching. As per the Kinnunen and Nylander model [13] and as per a rational model developed by Marzouk and Hussein [36], equilibrium equations can be developed in the vertical direction, horizontal direction, and due to the moment developed due to the individual forces acting at their respective distances from the column face.

The equation for equilibrium in the vertical direction determines Pult, the ultimate punching shear load. Since it is this quantity which is of interest, the equation for vertical equilibrium will be examined in greater detail.

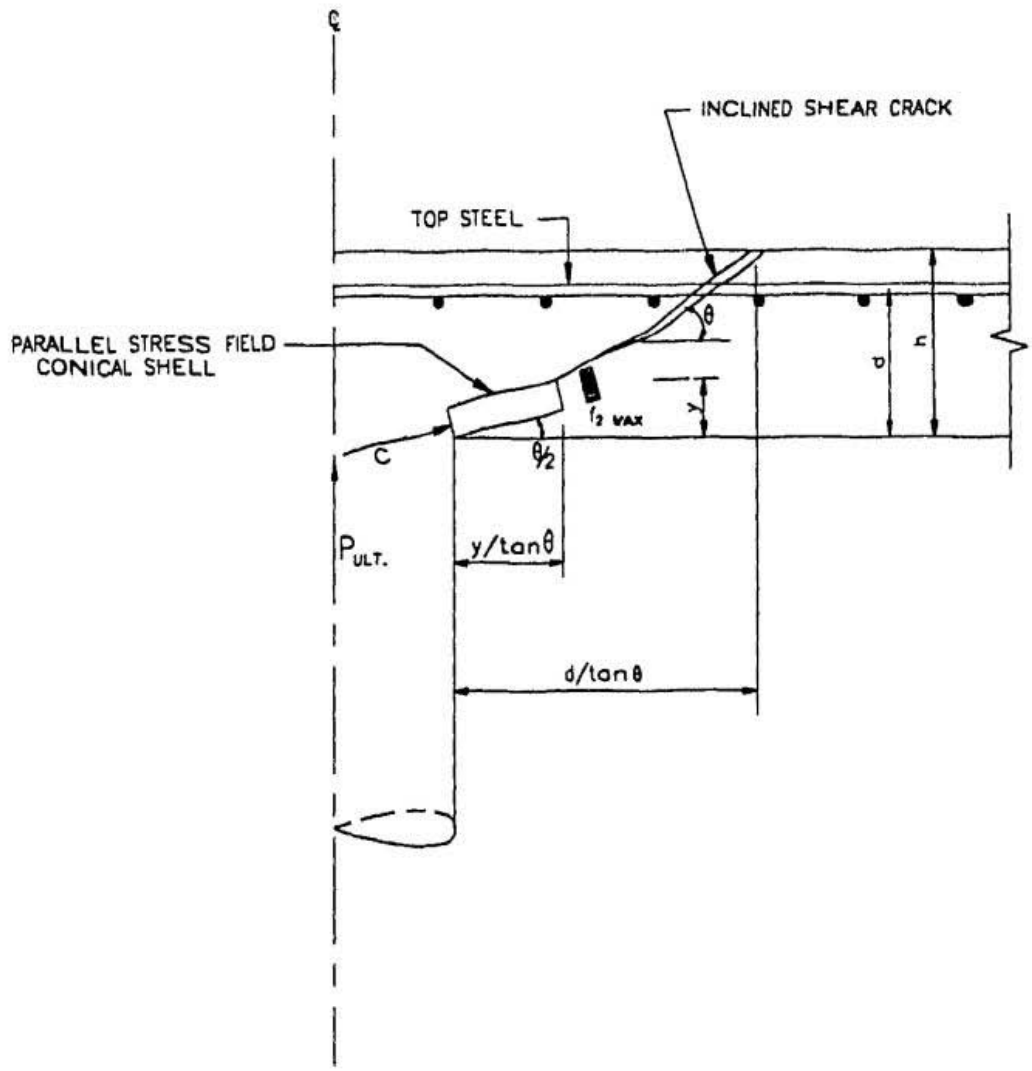

Figure 4.4: High radial compression stress failure mechanism.

The ultimate punching load, Pult, can be determined from the maximum concrete stress, f_{c2} max acting on the thickness of the conical shell-strut. This can be expressed as total compression force, C, around periphery of the circular column equals the bearing area of the conical shell-strut periphery multiplied by the maximum concrete strength allowed in the strut.

$C =$ Periphery bearing area $\times$ concrete strength, or
$C =$ (perimeter of cone $\times$ thickness of strut face) $\times$ concrete strength,

where

$$\text{perimeter of cone} = \pi(B + \frac{2y}{\tan\theta}),$$

$$\text{thickness of strut face} = \frac{y \sin\theta/2}{\sin\theta},$$

$$\text{concrete stress} = f_{c2}\,\text{max as per Equation 3.8.}$$

$$C = \frac{\text{Pult.}}{\sin\theta/2} = \left[\pi(B + \frac{2y}{\tan\theta}) \cdot \frac{y \sin\theta/2}{\sin\theta}\right] \cdot f_{c2}\,\text{max} \cdot S.E.$$

Solving for Pult.

$$\text{Pult} = \pi\left(B + \frac{2y}{\tan\theta}\right) \cdot \frac{y \sin\theta/2}{\sin\theta} \cdot f_{c2}\,\text{max} \cdot S.E. \cdot \sin\frac{\theta}{2} \tag{4.3}$$

If a square column is present, it can be replaced in the equation by an equivalent circular column with the same perimeter

$$B = \frac{4c}{\pi}$$

The factor $S.E.$ is introduced to account for size effects as recognized by Regan and Braestrup [33] and Broms [2]. Rather than take an empirical approach as performed by the above authors, it was decided that size effects should reflect a rational approach. The concept of the characteristic length, ℓ_{ch} of concrete as based on fracture

mechanics of concrete was selected as the rational approach [56]. Using results from recent research conducted by Abdel-Razek [56] at Memorial University of Newfoundland,

$S.E = \left(\frac{h}{\ell_{ch}}\right)^{-0.35}$

ℓ_{ch} = characteristic length of concrete, 500 for normal strength concrete, 250 for high strength concrete

h = slab thickness, mm

f'_c = cylinder strength, Mpa

The height of the parallel stress compression zone, y is determined based on the position of the neutral axis in a reinforced concrete flexural member under elastic conditions.

First, the critical section for flexure, b, is determined as per clause 13.3.3.3 of CAN3 A23.3-M84 [53]

$$b = B + 3h. \tag{4.4}$$

The depth of the rectangular compression block, a, can be determined by the following equation

$$a = \frac{\phi s A_s f_y}{0.85 \phi c f'_c b} \tag{4.5}$$

and the depth of the compression zone determined as

$$y = \frac{a}{\beta_1} \tag{4.6}$$

where

β_1 is a coefficient that depends on the strength of the concrete f'_c and can be found in clause 10.2.7 of the Canadian concrete code as

$\beta_1 = 0.85 - 0.008(f'_c - 30)$

A computer spreadsheet program was developed by the author to provide a quick determination of the ultimate punching shear load for a slab based on this approach. The source code and verification of this spreadsheet called "PUNCH" can be found in Appendix A. Comparison of the ultimate punching shear capacity of a concrete slab to experimental test results and the present Canadian concrete code equation can be found in Section 5.2.

4.1.4.2 Failure Modes

The general relationship between the load and the deflection of a concrete slab is illustrated in Figure 4.5.

Pure punching takes place when the flexural reinforcement ratio is very high and the reinforcement does not reach its yield value at any point in the slab (Curve 1).

Pure flexural failure (Curve 3) takes place in slabs with relatively low reinforcement ratios leading to the yielding of all reinforcement before punching occurs. Even in this case, however, sudden failure takes place when the ultimate concrete strain is reached near the column. Curve 2 illustrates the intermediate case in which part of the flexural reinforcement yields before punching occurs.

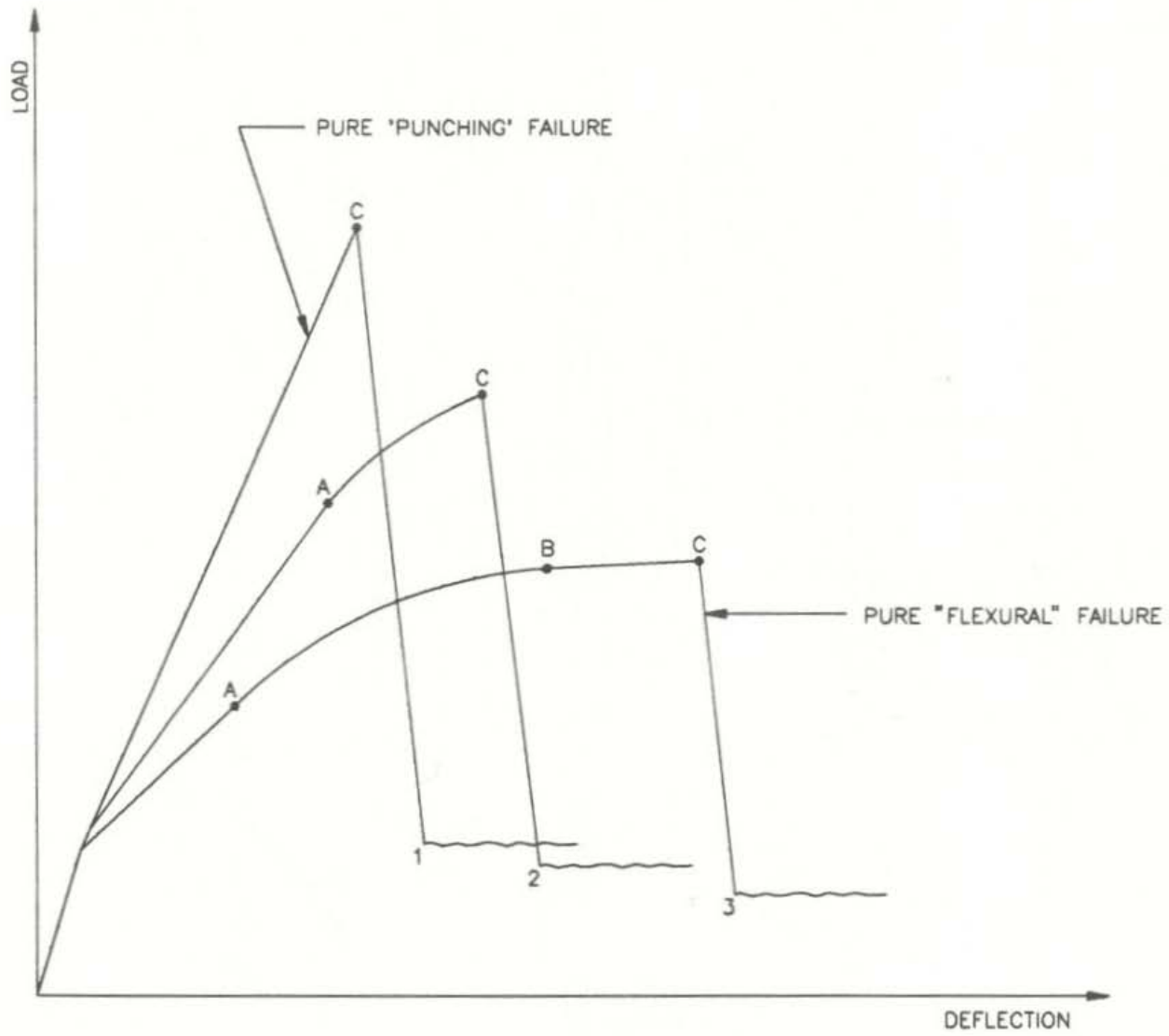

Figure 4.5: Failure modes.

4.2 Nonsymmetric Punching Shear of Concrete Slabs

4.2.1 Introduction

Lateral loads, as well as unbalanced gravity loads, cause transfer of moments between the slab system and supporting columns in slabs without beams along the column line; the transfer of the moment from the slab to the column requires special consideration. North American design codes specify that a portion, M_{fb}, of the total unbalanced moment, M_f, be considered as transferred to the columns by flexure; and the balance, M_{fv}, through shear and torsion, as given in Eqs. 4.7, 4.8, 4.9, and shown in Figure 4.6.

$$M_{fb} = \gamma_f M_f \tag{4.7}$$

$$M_{fv} = (1 - \gamma_f) M_f \tag{4.8}$$

$$\gamma_f = \frac{1}{\sqrt{\frac{c_1+d}{c_2+d}}} \tag{4.9}$$

where

$M_{fb} =$ portion of moment transferred by flexure
$M_{fv} =$ portion of moment transferred by shear
$M_f =$ total unbalanced moment transferred to columns
$c_1, c_2 =$ the size of equivalent rectangular column, measured in the direction moments are being determined, and transverse to it, respectively.

For square and round columns, $\gamma_f = 0.6$. Based on test results and experience, the width of slab considered effective in resisting the moment M_{fb} is taken as the width between lines a distance 1.5 h on either side of the column or column capital, and hence, this strip should have adequate flexural reinforcement to resist this moment. The section considered for moment transfer by eccentricity of shear stress is at a distance $d/2$ from the periphery of the column or column capital. The shear stresses

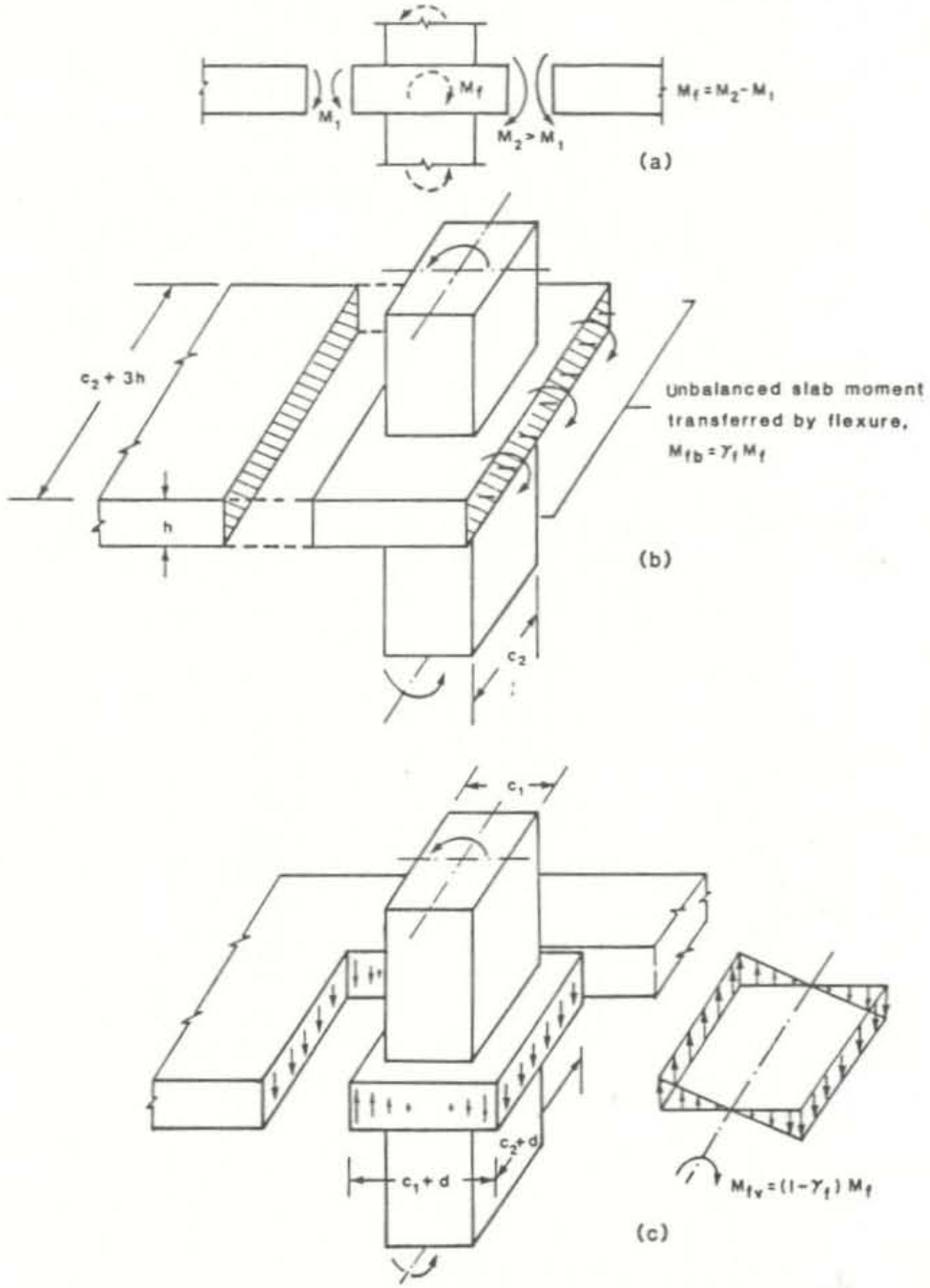

Figure 4.6: Transfer of unbalanced moment.

are introduced because of the moment transfer must be added to the shear stresses due to the vertical support reaction.

4.2.2 Strut-and-Tie Approach – Concrete Slabs

The strut-and-tie model developed earlier to model symmetric loading situations is used in conjunction with an interaction equation to describe nonsymmetric punching shear behaviour due to moment transfer. The interaction equation approach has been used in the past by Siao [46] and Broms [2].

The proposed interaction equation is given by the following:

$$\frac{P}{P_{ult}} + \frac{P(e)}{M_{ult}} \leq 1.0 \tag{4.10}$$

where

P	=	applied shear force
Pult	=	ultimate punching shear failure load as determined in section 4.1
e	=	eccentricity of applied shear force
Mult	=	ultimate moment resistance of slab
	=	moment resistance due to flexure, Mrb+ moment resistance due to shear stress acting at the critical section, Mrv.

$$\begin{aligned} M_{rb} &= \text{moment resistance of slab due to flexure} \\ M_{rb} &= (As - A's)fy(d - \tfrac{y}{2}) + A'sfy(d - d') \\ M_{rv} &= \text{moment resistance of slab due to shear} \\ M_{rv} &= \gamma_v \cdot M_0 \end{aligned} \tag{4.11}$$

where

$$\begin{aligned} \gamma_v &= 1 - \left(1 + \tfrac{2}{3}\sqrt{\tfrac{(c_1+d)}{(c_2+d)}}\right)^{-1} \\ &= 0.4 \text{ for a square column.} \end{aligned} \tag{4.11a}$$

$$M_0 = \frac{v_c J_1}{0.5(c_1 + d)} \cdot \frac{1}{\gamma_v} \tag{4.11b}$$

γ_v, J_1, c_1 and c_2 are explained in Section 2.1.5 of this report and v_c = shear strength (stress) of concrete.

$$M_{ult} = (Mrb + Mrv). \tag{4.12}$$

The eccentricity e, can be determined by dividing the applied moment by the shear force. Comparison of this strut-and-tie and interaction approach to experimental test results performed by others and the present Canadian concrete code can be found in Section 5.3. The computer program, "PUNCH," includes the above equations for nonsymmetric punching.

4.3 Concrete Slabs With Shear Reinforcement

4.3.1 Introduction

Shear reinforcement can be placed in the transverse direction in a slab at the column interface as shown in Figure 4.7. Several types of shear reinforcing can be used, these include (a) closed stirrups, (b) lapped hairpins, (c) open stirrups with end hooks, (d) nail-head-anchored stirrups, and (e) headed stirrups, see Figure 4.8.

The transverse reinforcement must be fully developed at the bottom and at the top to be effective. This is not an easy task, especially for thin slabs. It is clear that, apart from the anchorage requirement, a reasonably close spacing of the transverse reinforcing units is necessary.

Transverse reinforcement is cumbersome to place unless it is suitably detailed. Careful planning of the reinforcing cages is recommended when using closed stirrups. Rows of stirrups can be laid and placed as stable units into which the in-plane reinforcement can be fitted later. Nailhead-anchored stirrups can be inserted after having placed the in-plane reinforcement in the usual manner, while the headed studs are positioned prior to placing the in-plane reinforcement.

In the vicinity of concentrated loads of reactions, fan-shaped stress fields can develop in the core of the slab, as shown in Figure 4.7. In such cases, the transverse reinforcement within a ring-shaped zone of width $d \cdot \theta$ around the loaded area has to resist the integral of the transverse shear forces at the outer edge of the ring.

4.3.2 Shear Stud and T-Headed Reinforcement

In the past, punching shear reinforcement was seldom used in concrete slabs because of rebar congestion and because it was difficult to anchor these bars in the relatively

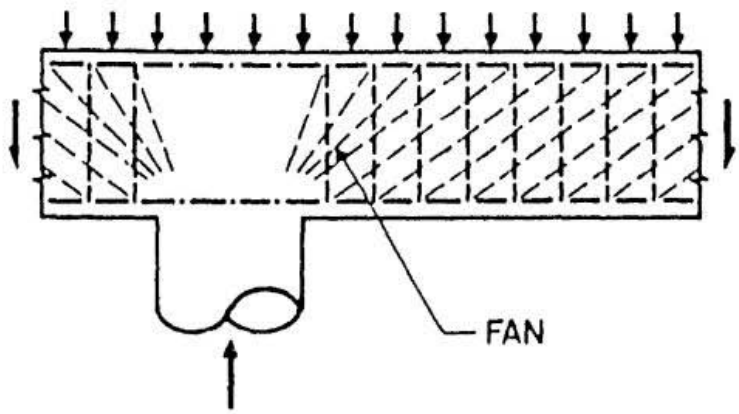

Figure 4.7: Punching shear reinforcement showing compression fans.

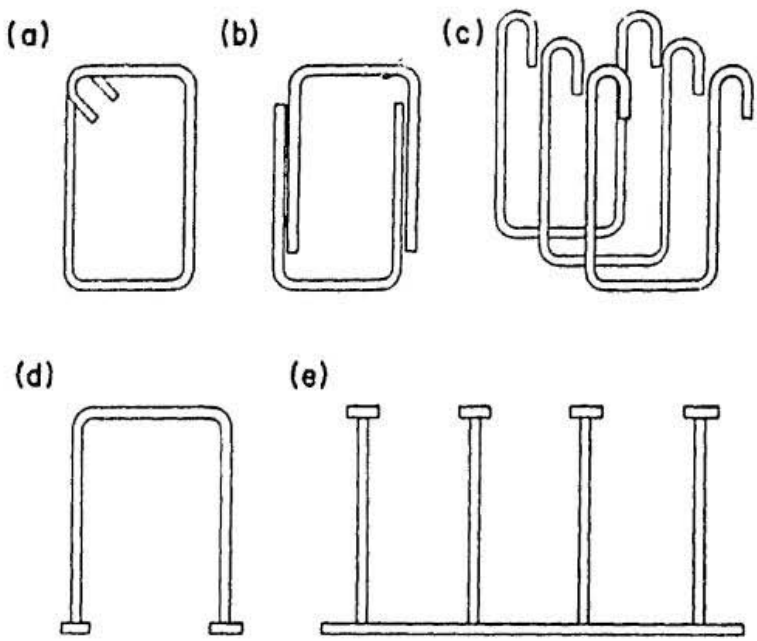

Figure 4.8: Types of punching shear reinforcement.

thin depths of most slabs. Figure 4.9 shows a relatively new type of punching shear reinforcement - the shear stud or t-headed bar. It is made up of vertical bars with anchor heads at the top. Often a steel strip bar is provided at the bottom. This system is secured in place before the top and bottom flexural bars are placed, thus reducing the congestion problem. The placing arrangements of these stud strips at an interior column location is shown in Figure 4.10.

The effectiveness of this type of shear reinforcement has been verified by extensive testing and experimentation [40, 41, 42] and is permitted in North American concrete codes.

4.3.3 Strut-and-Tie Model for Symmetric Loaded Concrete Slabs With Punching Shear Reinforcement

The proposed strut-and-tie model for a concrete slab with punching shear model consists of decentered fan shaped compression struts oriented at angles $\theta = 25°$ to $65°$ [43]. Therefore, shear reinforcement is effective for a distance $2d$ from the face of the column. The shear reinforcement bars act as vertical tension ties in the model. The top tension tie (flexural reinforcing bars) effectively anchor the horizontal component of the fanned struts. Nodal zones are developed at the intersection of the struts and ties.

The strut-and-tie model is solved by calculating P_{eq}, the equivalent force resulting from the load on the slab. The true strut-and-tie model for this situation extends around the periphery of the column in a three-dimensional cone shape. However, it is proposed for simplicity to solve the strut-and-tie model in a two-dimensional manner, therefore, P_{eq} is based on a contributing width effective to each row of punching shear reinforcement.

The force, P_{eq}, is distributed to each compression fan. Concrete design criteria is

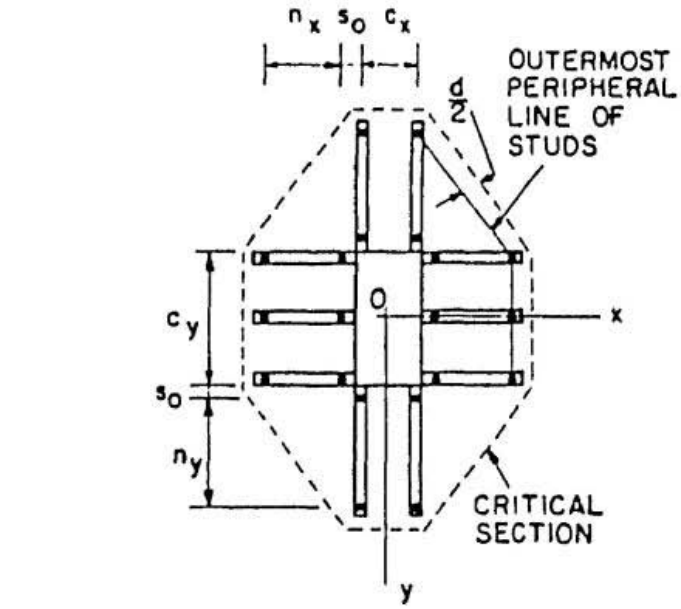

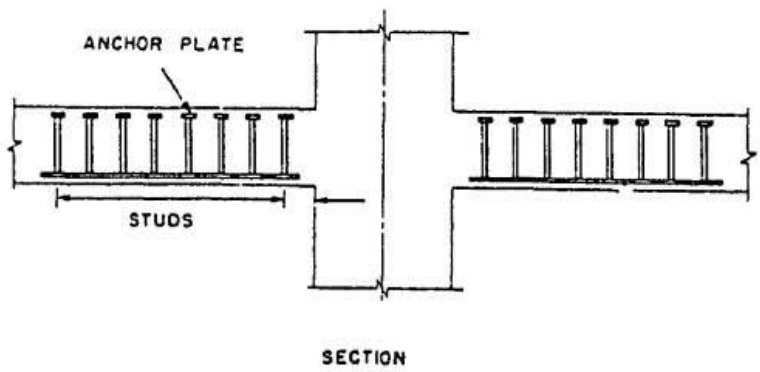

Figure 4.9: Shear studs and arrangement around an interior column (adapted from [41]).

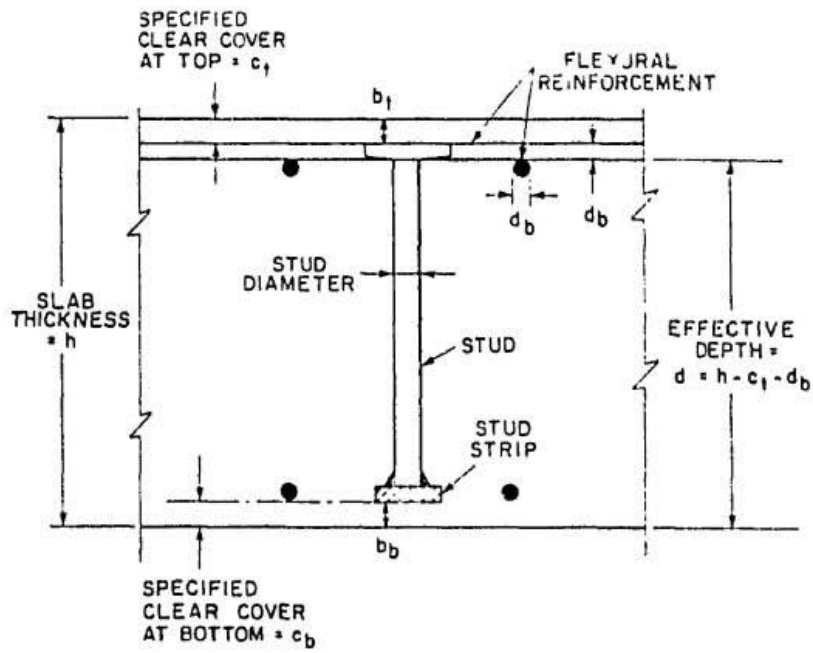

Figure 4.10: Punching shear studs (adapted from [40]).

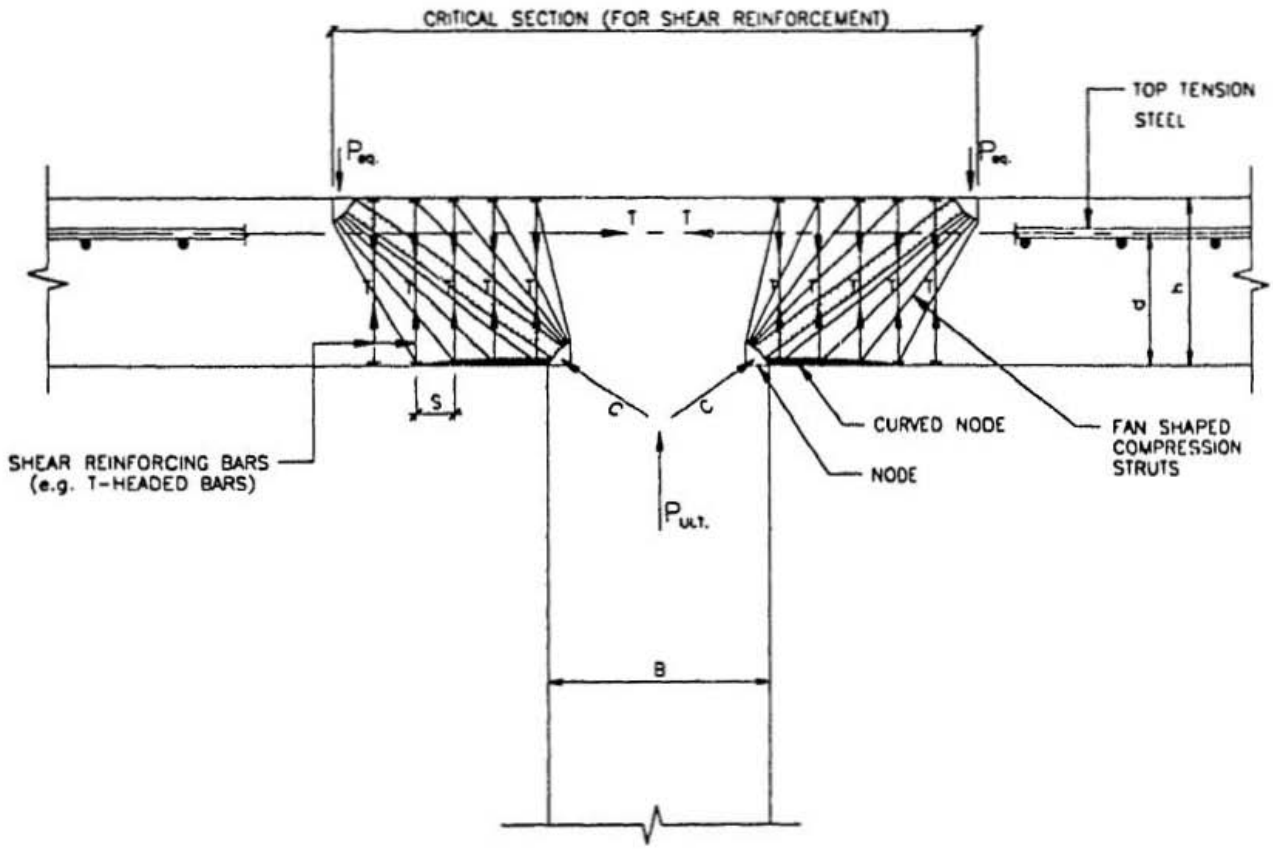

Figure 4.11: Strut-and-tie model for punching shear with punching reinforcement.

checked for these elements along with the nodes and ties based on accepted criteria such as the Canadian design code criteria described in section 3.4. Pult, the ultimate punching shear failure load of the slab system can be determined when either one of the basic strut-and-tie elements (i.e., compression strut fans, tension ties or node elements) reach failure criteria. The analysis procedure can be simplified by taking advantage of clause 11.4.7.7 of CAN3 A23.3-M84 [53]. This clause states that in regions of 'fan shaped' compression struts the concrete design criteria of clause 11.4.7.3 and 11.4.7.5 may be considered satisfied if the requirements of clause 11.4.7.6 (c) is satisfied. The latter clause states that the compressive stress limits of all components in the strut-and-tie model are satisfied if the tension reinforcement (top flexural bars) is anchored over a sufficient width that the tension force results in a stress in the top node of less than $0.75\phi_c f'_c$. refer to Figure 1.11. From this basis, the top nodal zone can be checked for high compressive stress. It has been documented [45] from test results that ultimate failure occurs most often at the bottom node adjacent to the column. This failure is due to the compressive stress acting over the width of the node exceeding f_{c2} max (f_{c2} max in this situation can be taken as $0.85\phi_c f'c$). The depth of the nodal zone, y, can be approximated from elastic flexure theory as

$$y = \frac{\phi_s As \cdot Fy}{0.85 \cdot \phi_c f'_c \cdot b} \tag{4.15}$$

As per the equilibrium requirements of Section 3.2.3.4 of this report, the height of the top nodal zone must equal the height of the bottom nodal zone. Therefore, ultimate punching shear failure is considered at the bottom node and checked at the top node.

Following the above approach, the strut-and-tie model for punching shear of a concrete slab with punching shear reinforcement was compared to test results performed and published by others. The results and comparisons are shown in Section 5.4.

Chapter 5

Comparison of Strut-and-Tie Model With Test Results

5.1 Introduction

This section summarizes the results using the strut-and-tie model developed in the previous chapter for punching resistance shear of concrete slabs. These results are compared to published results on normal and high strength concrete slabs reported by others in past literature.

5.2 Symmetric Punching Shear of Concrete Slabs

Table 5.1 and Figures 5.1, 5.2, 5.3, 5.4, summarizes the results of the strut-and-tie model for symmetric punching compared to published test results and the present Canadian concrete code, CAN3 A23.3-M84 [53], equation.

Two parameters can be used to compare the strut-and-tie results to the Canadian code; concrete strength f'_c and reinforcing ratio, ρ. The strut-and-tie results are approximately the same as Canadian code results for low strength concrete less than 20 Mpa results. The strut-and-tie results have an average ratio of 0.80 compared to test results whereas the code has a value of 0.82. For normal strength concrete between 20 and 40 Mpa, the results for the strut-and-tie model are again generally the same as the Canadian code results. In high-strength concrete applications, greater

than 40 Mpa, the strut-and-tie results (average ratio of 1.09) are significantly closer to the test results than the code results are (average ratio of 0.85). Generally, these results are in agreement with the fact that the Canadian code is based on an empirical equation directly related to concrete strength, and for all intents and purposes, is only applicable for concrete less than 40 Mpa in strength. The strut-and-tie model, however, is a rational model based on the actual slab-column behaviour.

The effect of the amount of top flexural steel, i.e., the reinforcing ratio, ρ, will now be examined. The Canadian code equation of Clause 11.10.2 of CAN3 A23.3-M84[53] has no provision for the reinforcing ratio, ρ. The strut-and-tie model, however, is affected by the reinforcing ratio, ρ. As the reinforcing ratio, ρ, of the test slabs increase, the failure mode goes from a "ductile" type failure to a "sudden"-"pure punching" type failure. Generally, for the test results with high reinforcement ratios, ρ, the strut-and-tie results are almost identical to the test results with an average ratio of 0.99 whereas the Canadian code results have an average ratio of 0.84.

The result, in summary, indicate that the strut-and-tie model has excellent results for low, normal, and high strength concrete and for low and high reinforcing ratios. The current Canadian code equation only has good results for normal strength concrete with low reinforcing ratios. As a result, the strut-and-tie model would have applications in the offshore where high strength concrete and high reinforcing ratios are quite common.

Table 5.1 – Strut–and–Tie Model for Symmetric Punching Shear: Comparison with Published Test Results and Canadian code.

Authors	Slab No.	d (mm)	Col Size,c (mm)	r3 (mm)	rho (%)	f'c (Mpa)	fy (Mpa)	Vc CSA (kn)	Strut–and–Tie Pult (kn)	P Test (kn)	Vc CSA / P Test	Pult STM / P Test
Elstner and	A–1(a)	116	254	1780	1.15	14.1	332	257.9	251	302	0.85	0.83
Hognestad	A–1(e)	116	254	1780	1.15	20.3	332	309.4	246	356	0.87	0.69
1956, [10]	A–1(b)	116	254	1780	1.15	25.2	332	344.7	306	365	0.94	0.84
	A–1(d)	116	254	1780	1.15	36.8	332	416.6	398	351	1.19	1.13
	A–4	116	254	1780	1.18	26.1	332	350.8	317.0	400	0.88	0.79
	B–9	114	254	1780	2.00	43.9	341	444.7	504.0	505	0.88	1.00
	B–11	114	254	1780	3.00	13.5	410	246.6	280.0	329	0.75	0.85
	B–14	114	254	1780	3.00	50.5	325	477.0	628.0	578	0.83	1.09
	A–11	114	356	1780	2.47	25.9	332	436.3	575.0	529	0.82	1.09
										Average:	0.89	0.92
										Standard Deviation:	0.12	0.15
Kinnunen	5	117	150	1710	0.80	33.5	441	227.2	310.0	255	0.89	1.22
& Nylander	6	118	150	1710	0.79	32.8	454	227.6	293.0	275	0.83	1.07
1960, [13]	24	128	300	1710	1.01	33.0	455	395.5	486.0	430	0.92	1.13
	25	124	300	1710	1.04	31.4	451	370.2	450.0	408	0.91	1.10
	32	123	300	1710	0.49	32.9	448	375.0	240.0	258	1.45	0.93
	33	125	300	1710	0.48	33.3	462	385.2	242.0	258	1.49	0.94
										Average:	1.08	1.06
										Standard Deviation:	0.28	0.10
Marzouk												
& Hussein	HS2	95	150	1700	0.84	70	490	311.6	338.0	221	1.41	1.53
1991, [36]	HS7	95	150	1700	1.19	74	490	320.4	463.0	356	0.90	1.30
	HS3	95	150	1700	1.47	69	490	309.3	431.0	356	0.87	1.21
High	HS4	90	150	1700	2.37	66	420	280.8	413.0	418	0.67	0.99
Strength	HS6	120	150	1700	0.94	70	490	433.7	533.0	489	0.89	1.09
Concrete	HS8	120	150	1700	1.11	69	420	430.6	525.0	436	0.99	1.20
	HS9	120	150	1700	1.61	74	420	445.9	563.0	543	0.82	1.04
	HS10	120	150	1700	2.33	80	420	463.7	610.0	645	0.72	0.95
	HS11	70	150	1700	0.95	70	490	206.2	198.0	196	1.05	1.01
	HS12	70	150	1700	1.52	75	490	213.4	281.0	258	0.83	1.09
	HS13	70	150	1700	2.00	65	490	198.7	322.0	267	0.74	1.21
	HS14	95	220	1700	1.47	72	490	406.3	582.0	498	0.82	1.17
										Average:	0.82	1.06
										Standard Deviation:	0.19	0.15
Marti et. al.	P2	145	300	2600	1.44	43.3	558	533.6	560.0	600	0.89	0.93
1983,[37]	P5	154	300	2600	1.34	32.8	515	503.2	592.0	569	0.88	1.04
										Average:	0.89	0.99
										Standard Deviation:	0.002	0.05

Notes:

1. Results from Spreadsheet "PUNCH"
2. Vc CSA = 0.4*sqrt(f'c)*(bo)*d, (Clause 11.10.2 CAN A23.3-M84)

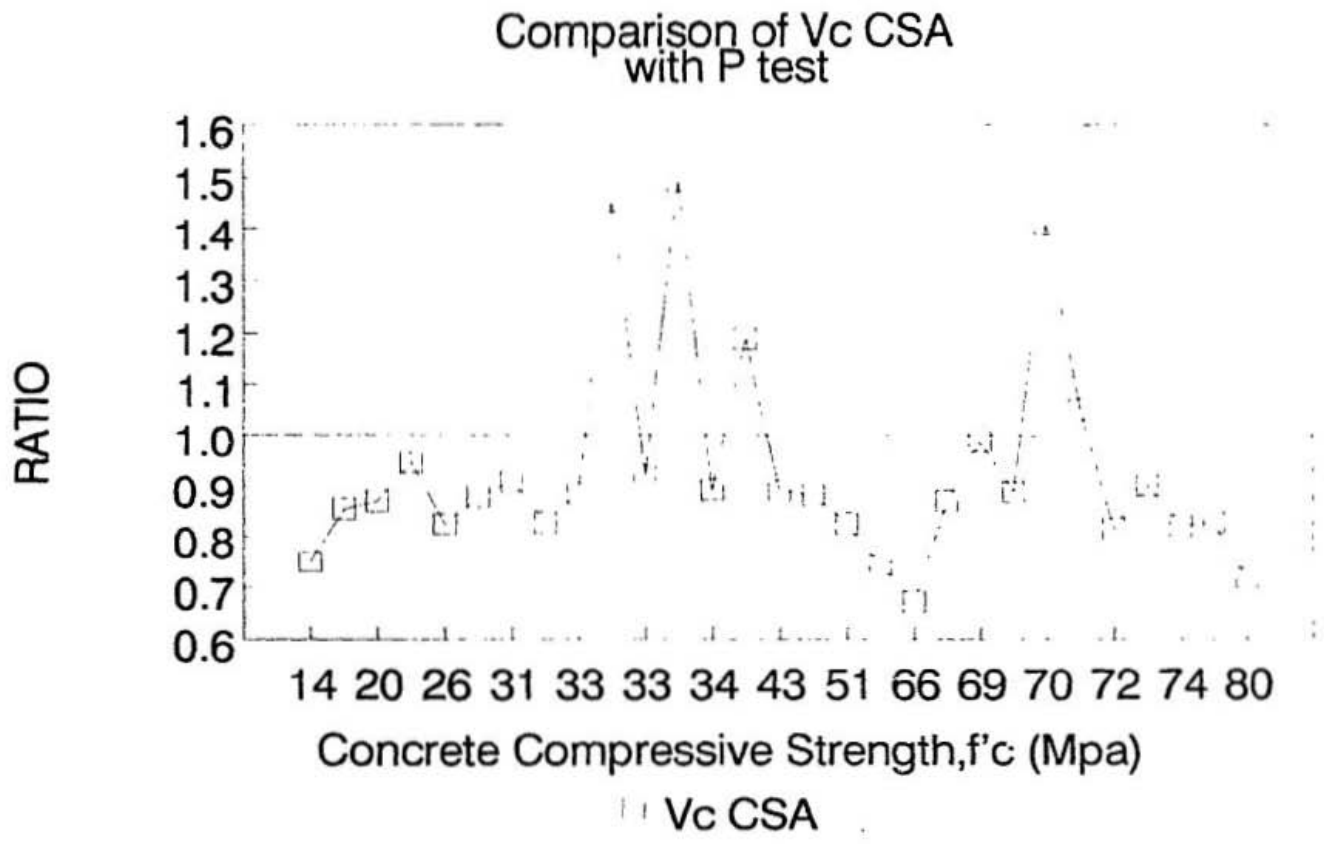

Figure 5.1 **Symmetric Punching Shear Comparison Canadian Code vs Test Load**

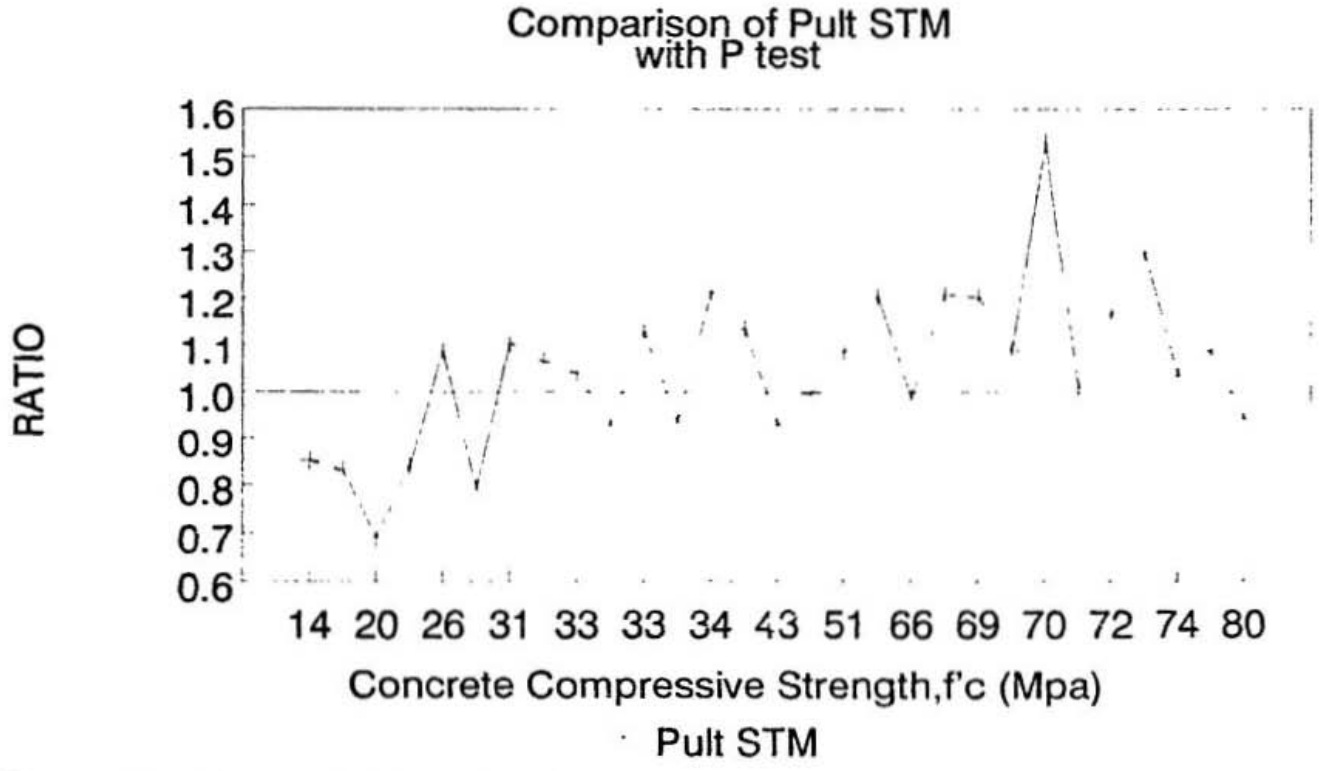

Figure 5.2 Symmetric Punching Shear Comparison Strut–and–Tie Model vs Test Load

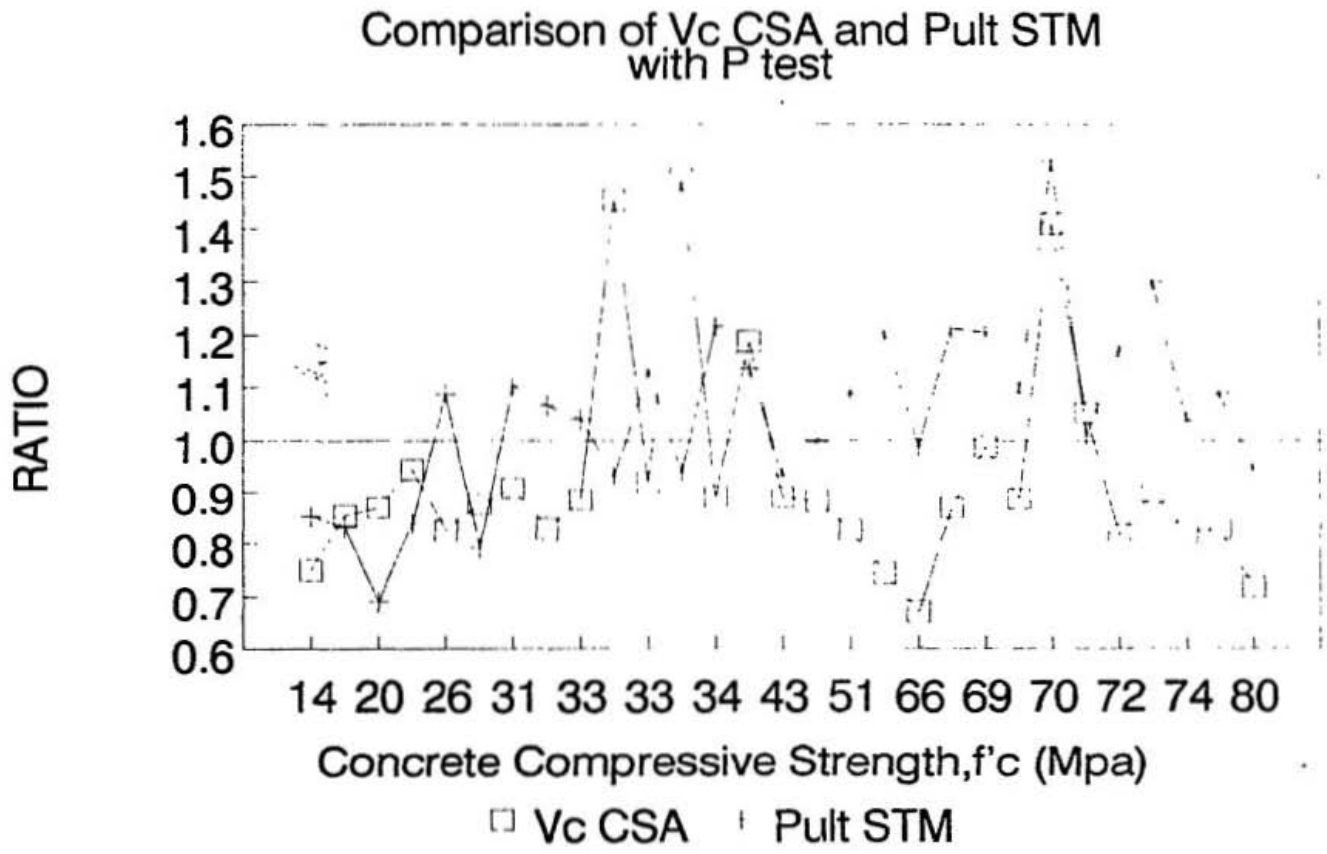

Figure 5.3 Symmetric Punching Shear Comparison

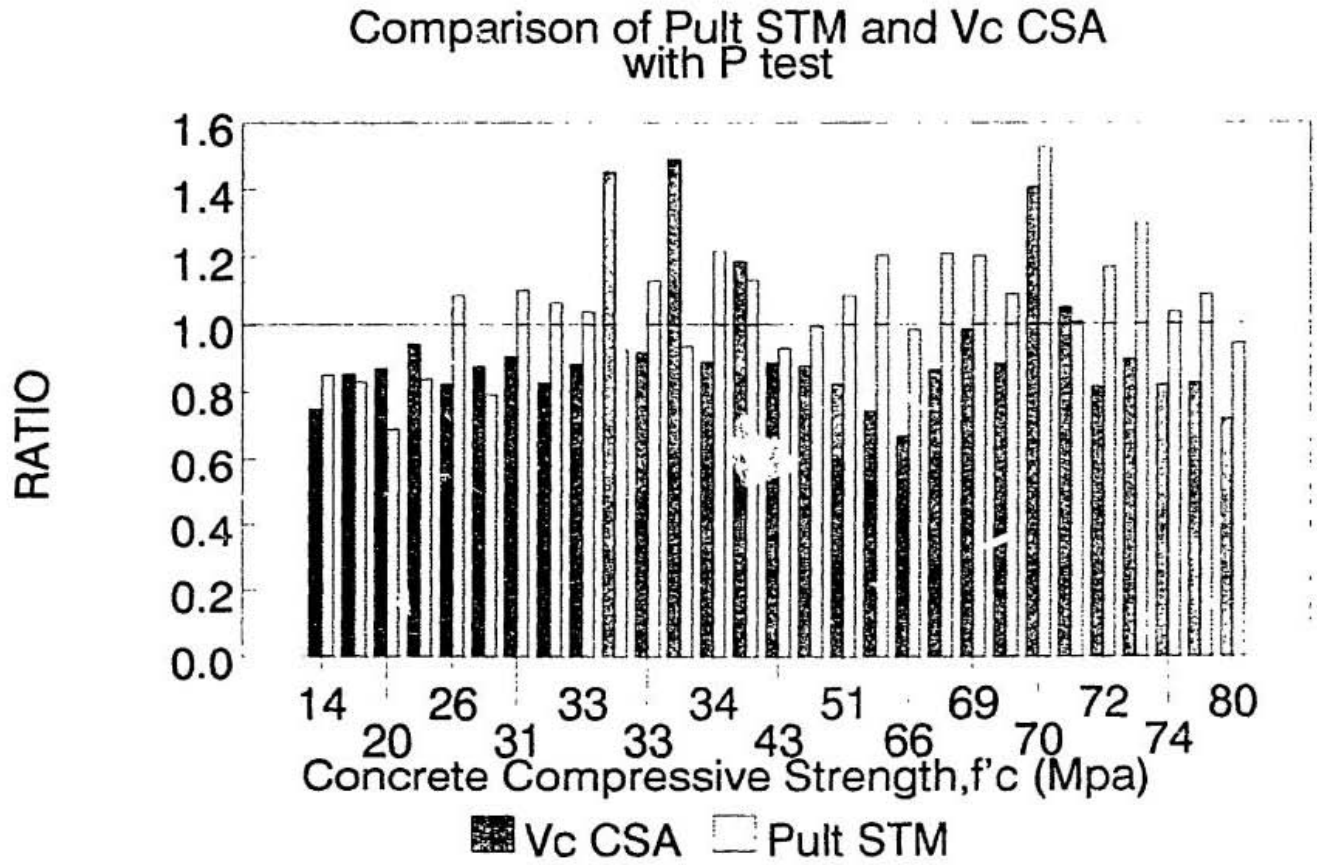

Figure 5.4 Symmetric Punching Shear Comparison

5.3 Nonsymmetric Punching Shear of Concrete Slabs

Table 5.2 summarizes the results of the proposed interaction equation approach developed for this situation of nonsymmetric punching shear compared with published test results by others.

5.3.1 Test Results – Nonsymmetric Punching

The strut-and-tie model in conjunction with the interaction equation approach yields excellent results when compared to the test values. The maximum allowable applied load, P, has an average value of 0.95 when compared to fifteen (15) reported test results. The strut-and-tie approach was, as per the symmetric loading situation, comparable to test results over the full range of concrete strengths and reinforcing ratios indicated. The comments found in Section 5.2 apply to nonsymmetric punching shear applications. The Canadian code CAN3-A23.3-M84[53] does not treat nonsymmetric punching shear through an interaction equation. As a result, no comparisons to the Canadian code where applicable.

The results, in summary, indicate that the strut-and-tie model in conjunction with the interaction equation rationally describes the punching behaviour of a slab under the application of a load at an eccentricity. Excellent results are shown for low, normal, and high strength concrete test slabs for ductile and non-ductile punching situations.

Table 5.2– Strut–and–Tie Model for Non–Symmetric Punching Shear: Comparison with Published Test Results.

Authors	Slab No.	d (mm)	Col Size,c (mm)	rho (%)	f'c (Mpa)	fy (Mpa)	e (mm)	Pult Strut–&–Tie (kn) 1	Mult (kn–m)	P (kn)	P test (kn)	P/P test
Moe	M2A	114	305	1.50	15.5	481	185	287	110	193	213	0.91
1961, [11]	M7	114	254	1.34	25.0	328	61	377	75	289	311	0.93
	M6	114	254	1.34	26.5	328	168	382	76	207	239	0.87
	M8	114	254	1.91	24.6	328	437	425	97	146	150	0.97
	M10	114	254	1.91	21.1	328	307	366	94	167	178	0.94
											Average:	**0.92**
											Standard Deviation:	**0.04**
Ghali et. al.	SM1.5	122	305	2.00	39.9	476	1031	612	198	146	129	1.13
1987, [47]	SM1.0	122	305	1.33	33.4	476	988	548	136	110	129	0.85
											Average:	**0.99**
											Standard Deviation:	**0.14**
Marzouk,Enam	NNH S1.0	125	250	1.00	36.2	460	550	472	100	131	130	1.01
& Hilal [44]	NHH S1.0	125	250	1.00	35.3	460	550	468	100	130	135	0.96
											Average:	**0.99**
											Standard Deviation:	**0.02**
Hawkins et al	6AH	133	305	0.60	31.3	472	584	480	98	125	169	0.74
1989, [55]	9.6AH	133	305	0.96	30.7	415	584	471	116	140	187	0.75
	14AH	133	305	1.40	30.3	420	584	470	143	161	205	0.79
	6AL	133	305	0.60	22.7	472	130	348	92	233	244	0.95
	9.6AL	133	305	0.96	28.9	415	130	445	115	296	257	1.15
	14AL	133	305	1.40	27.0	420	130	464	139	323	319	1.01
											Average:	**0.90**
											Standard Deviation:	**0.15**

Notes:

1. Results from Spreadsheet "PUNCH"

5.4 Punching Shear of Concrete Slabs With Punching Shear Reinforcement

Table 5.3 summarizes the results of the proposed strut-and-tie model compared to experimental test results performed by others. Test results used were for either shear studs or *T*-headed bars since these are considered to be the only practical shear reinforcement types to be used in concrete slab construction.

5.4.1 Test Results – Punching Shear Reinforcement

For the limited test results examined the ultimate punching shear load as calculated by the strut-and-tie model showed excellent results when compared to the test results The Canadian code, CAN3 A23.3-M84[53] does not provide any direct means of calculating the punching shear capacity of a slab utilizing *T*-headed bars. The strut-and-tie approach developed borrows from some of the basic concrete failure criteria for strut-and-tie models and indicates excellent results for normal and high strength concrete test slabs.

In summary, the strut-and-tie model for punching shear behaviour of slabs with shear reinforcing is a rational model based on the actual slab-reinforcing behaviour. It is an effective and practical means of analyzing slabs with punching shear reinforcing.

Table 5.3 – Strut–and–Tie Model: Comparison with Published Test Results

Authors	Slab No.	f'c (Mpa)	fv (Mpa)	Shear Reinforcing Type	Pult Strut–&–Tie (kn)	P test (kn)	Pult Ptest
Van der Voet	MV2	29.5	331	Tee Headed	560	602	0.93
Dilger and	MV4	31.3	344	Tee Headed	594	588	1.01
GHALI [45]	MV5	36.5	339	Tee Headed	672	592	1.14
						Average:	1.03
Jiang and	HS22	60	450	Tee Headed	576	605	0.95
Marzouk[43]	HS23	60	450	Tee Headed	576	590	0.98
						Average:	0.96

Chapter 6

Conclusions

6.1 General

Punching shear failure of concrete slabs is an important consideration in design. Current equations in North American codes are empirically based and shed very little light on the actual mechanism of punching shear behaviour and failure. These equations have been developed for concrete with compressive strengths between 14-40 Mpa. They do not adequately cover high strength concrete applications.

Strut-and-tie models present a unified, consistent, rational, and simplified, model for the behaviour of concrete elements. The phenomena of punching shear behaviour of concrete slabs of various compressive strengths can be adequately modelled using strut-and-tie models.

For symmetric loading situations, the punching shear behaviour can be modelled using a strut-and-tie model. The ultimate punching slab capacity can be predicted using elastic theory equations based on the classic Kinnunen and Nylander plate theory rational model [13] and concrete failure criteria and is adjusted for size effects.

In nonsymmetric loading situations, the strut-and-tie model used to describe symmetric punching is used in conjunction with an interaction equation to model the punching behaviour.

A strut-and-tie model consisting of fan-shaped compression struts held in place by tension ties can be used to describe the situation where punching shear reinforcement

is present. The proposed strut-and-tie models for punching shear compare quite well with experimental test results. For symmetric punching, the proposed equation has an average of 0.92, 1.06, 1.06, and 0.99 when compared to four separate sets of experimental test results. For nonsymmetric punching shear, the proposed approach has averages of 0.92, 0.99, and 0.99, and 0.90 when compared to four separate test programs. Finally, the strut-and-tie model for concrete slabs with shear reinforcement has averages of 1.03 and 0.96 when compared to two separate test programs. Simple computer programs can be developed to assist the designer in the sometimes tedious and repetitive calculations involved in these strut-and-tie models. An example of this is the spreadsheet program developed by the author for symmetric loaded situations.

The work done in this investigation could be expanded to include other punching shear situations in slabs. These include exterior column situations in building construction, different types of slab systems such as flat slabs with drop panels, punching shear for offshore concrete structures and punching shear related to dropping objects on concrete slabs.

References

1. J. Moe, "Shearing Strength of Reinforced Concrete Slabs and Footings Under Concentrated Loads," *Development Department Bulletin D47*. Portland Cement Association, Skokie, April 1961.

2. C.E. Broms, "Punching of Flat Plates – A Question of Concrete Properties in Biaxial Compression and Size Effect," *Journal of the American Concrete Institute*, vol. 87, No. 3, May-June 1990, pp. 292-304.

3. A. Talbot, "Reinforced Concrete Wall Footings and Column Footings," Bulletin No. 67, University of Illinois, Engineering Experiment Station, March 1913.

4. O. Graf, "Strength Tests of Thick Reinforced Concrete Slabs Supported on All Sides Under Concentrated Loads," *Deutscher Ausschuss fur Eisenbeton*, No. 88, Berlin, Germany, 1938.

5. C. Forsell and A. Holemberg, "Concentrated Loads on Concrete Slabs," *Betong*, Vol. 31, No. 2, Stockholm, Sweden, February 1946, pp. 95-123.

6. E. Hognestad, "Shearing Strength of Reinforced Concrete Column Footings," *Journal of the American Concrete Institute*, Vol. 50, No. 3, November 1953, pp. 189-208.

7. F.E. Richart, "Reinforced Concrete Wall and Column Footings," *Journal of the American Concrete Institute*, Vol. 45, Nos. 2 and 3, October, November 1953, pp. 97-127-237-260.

8. R.C. Elstner and E. Hognestad, "An Investigation of Reinforced Concrete Slabs Failing in Shear," University of Illinois, Department of Theoretical and Applied Mechanics, 1953.

9. F.E. Richart and R.W. Kluge, "Tests of Reinforced Slabs Subjected to Concentrated Loads," *Bulletin 314*, University of Illinois, Engineering Experiment Station, 1939.

10. R.C. Elstner and E. Hognestad, "Shearing Strength of Reinforced Concrete Slabs," *Journal of the American Concrete Institute*, Vol. 53, No. 1, July 1956, pp. 29-58.

11. J. Moe, "Shearing Strength of Reinforced Concrete Slabs and Footings Under Concentrated Loads," *Development Department Bulletin D47*, Portland Cement Association, Skokie, April 1961.

12. ACI-ASCE Committee 316, "Shear and Diagonal Tension," *Proceedings*, American Concrete Institute, Vol. 59, January, February, and March 1962, pp. 1-30, 227-334, and 353-396.

13. S. Kinnunen and H. Nylander, "Punching of Concrete Slabs Without Shear Reinforcement," *Transactions No. 158*, Royal Institute of Technology, Stockholm, Sweden, 1960.

14. S. Kinnunen, "Punching of Concrete with Two-Way Reinforcement," *Transactions No. 198*, Royal Institute of Technology, Stockholm, Sweden, 1963.

15. A.E. Long, "Punching Failure of Reinforced Concrete Slabs," *Ph.D. Thesis*, Queen's University at Belfast, Northern Ireland, 1967.

16. H. Reimann, "Zur Bemessung von Dünne Plattendecken auf Stützen Ohne Kopf Gegen Durchstanzen" (Method for Calculating the Punching Load of Flat Slabs Supported by Columns Without Capitals"), *Dr. -Ing. Thesis*, Technischen Hochschule, Stuttgart, Germany, January 1963.

17. A. Long and D. Bond, "Punching Failure of Reinforced Concrete Slabs," *Proceedings of the Institute of Civil Engineers*, Vol. 37, May 1967, pp. 109-136. Discussion: *Proceedings of the Institute of Civil Engineers*, Vol. 39, June 1968, pp. 151-164.

18. D.M. Masterson and A.E. Long, "The Punching Strength of Slabs, A Flexural Approach Using Finite Elements," *SP 42 Shear in Reinforced Concrete*, American Concrete Institute, Detroit, 1974, pp. 747-768.

19. A.E. Long, "A Two-Phase Approach to the Prediction of the Punching Strength of Slabs," *Journal of the American Concrete Institute*, Vol. 72, No. 2, February 1975, pp. 37-47.

20. A.E. Long, "Predicting the Punching Strength of Conventional Slab Column Connections," *Proceedings of the Institution of Civil Engineering*, Vol. 82, April 1987, pp. 327-346.

21. H. Gesund and O.P. Dikshit, "Yield Line Analysis of the Punching Problem at Slab/Column Intersections," *SP-30, Cracking, Deflection and Ultimate Load of Concrete Slab Systems*, American Concrete Institute, Detroit, 1971, pp. 177-202.

22. H. Gesund and Y.P. Kaushik, "Yield Line Analysis of the Punching Failures in Slabs," *Publications, International Association for Bridge and Structural Engineering*, Zurich, Switzerland, Vol. 30-1, 1970.

23. M.P. Nielson, M.W. Braesturp, B.C. Jensen, and F. Bach, "Concrete Elasticity - Beam Shear - Punching Shear - Shear in Joints," *Danish Society for Structural Science and Engineering*, October 1978.

24. H. Andrä, "On the Strengths of Support Regions of Flat Slabs, (Zur Tragverhalten des Auflagerbereichs von Flachdecken)," *Ph.D. Thesis*, University of Stuttgart, Stuttgart, Germany, 1982.

25. I.A. Shehata, "Theory of Punching in Concrete Slabs," *Ph.D. Thesis*, Polytechnic of Central London, London, 1985.

26. I.M. Shehata and P. Regan, " Punching in R.C. Slabs," *ASCE, Journal of the Structural Division*, Vol. 115, No. 7, August 1989, pp. 1726-1740.

27. S.D. Alexander and S.H. Simmonds, "Ultimate Strength of Slab-Column Connections," *American Concrete Institute Structural Journal*, Vol. 184, No. 3, 1987, pp. 255-261.

28. W. Ritter, "Die Bauweise Hennebique," *Schweizerische Bauzeitung*, Bd. xxxiii, No. 7, January 1889.

29. E. Morsche, "Der Eisenbetonban, Seine Thedrie und Andwendung," *Verlag Konrad*, Witlever, Stuttgart, 1912.

30. J. Schlaich, K. Schafer, and M. Jennewein, "Towards a Consistent Design of Reinforced Concrete Structures," *Journal of the Prestressed Concrete Institute*, Vol. 32, No. 3, May-June 1987, pp. 75-150.

31. J. Schlaich and D. Wieschede, "Einpraktisches Verfarhren zum Methodischen Bemesson und Konstruierin in Stahlbetonban," *Bulletin d'Information No. 150*, CEB, Paris, March 1982.

32. B. Thurlimann, P. Marti, J. Pralong, P. Ritz, and B. Zimmerli, "Vorlesungum forbildungskurs für Bauingenieure," *Institute für Baustatik und Konstruktion*, Eth Zurich, 1983.

33. P.E. Regan and M.W. Braestrup, "Punching Shear in Reinforced Concrete: A State of the Art Report." *Bulletin d'Information No. 168*. CEB. Lausanne. 1985.

34. K. Wesche, "Baustoffe für Tragenoe Bauteile. Bano 2. Nichtmetallisch Anorganische Stoffe, Beton Mauerwerk," *Bauverlag GMBH*. Weisbaden and Berlin. 1974.

35. R.C. Elstener and E. Hognestad. "Shearing Strength of Reinforced Concrete Slabs," *Journal of the American Concrete Institute*. Vol. 53. No. 1. 1956. pp. 29-58.

36. H. Marzouk and A. Hussein. "Punching Shear Analysis of Reinforced High Strength Concrete Slabs," *Canadian Journal of Civil Engineering*. Vol. 18, 1991, pp. 954-963.

37. P. Marti, J. Pralong, and B. Thurlimann. "Punching Tests of Reinforced Concrete Slabs." *Bericht*, No. 7305-03, Institut fur Baustatik und Konstruktion. ETH, Zurich, Sept., 1977.

38. D.D. Magura and W.G. Corley, "Test to Destruction of a Multipanel Waffle Slab," *Full Scale Testing of New York World's Fair Structures*, Vol. 2, The Rathskeller Structure, National Academy of Science, Washington. D.C., 1969, pp. 10-135.

39. A.A. Hussein, "Behaviour of Reinforced Concrete Slabs Made With High Strength Concrete," Master of Engineering Thesis, Memorial University of Newfoundland, 1992.

40. A. Ghali, "An Efficient Solution to Punching of Slabs," *Concrete International*, June, 1989, pp. 50-54.

41. A. Ghali and A.A. Elgabry, "Design of Stud-Shear Reinforcement for Slabs," *American Concrete Institute, Structural Journal*, Vol. 87, No. 3, May-June 1990, pp. 351-361.

42. A. Ghali and N. Hammell, "Effectiveness of Shear Reinforcement in Slabs," *Concrete International*, January 1992, pp. 60-65.

43. D. Jiang, "Evaluation of Shear Enhancement for High Strength Concrete Plates," Master of Engineering Thesis, Memorial University of Newfoundland, 1994.

44. H. Marzouk, M. Emam, and S. Hilal, "Effect of High-Strength Concrete Column on the Behaviour of Slab-Column Connections," A paper to be published in 1995.

45. A.F. Van Der Voet, W.H. Dilger, and A. Ghali, "Concrete Flat Plates With Well-Anchored Shear Reinforcement Elements," *Canadian Journal of Civil Engineering*, Vol. 9, 1982, pp. 107-114.

46. W.B. Siao, "Punching Shear Resistance of Flat Slabs: A Beam-Strip Analogy," *American Concrete Institute, Structural Journal*, September-October 1994, pp. 594-603.

47. A. Ghali, and A.A. Elgabry, "Tests on Concrete Slab Column Connections with Shear-Stud Reinforcement Subjected to Shear-Moment Transfer," *American Concrete Insititute, Structural Journal*, Vol. 84, No. 5, September-October 1987, pp. 433-442.

48. R.M. Ellis and J.G. MacGregor. "Behaviour and Design of Reinforced Concrete Ice-Resisting Walls." Structural Engineering Report 162. University of Alberta. Department of Civil Engineering. November 1988.

49. H. Marzouk and Z. Chen. "Tension Softening Behaviour of High-Strength Concrete Made With Silica Fume and Fly Ash." a paper summarizing work done at Memorial University of Newfoundland. 1993.

50. F. Vecchio and M.P. Collins. "The Modified Compression - Field Theory for Reinforced Concrete Elements Subjected to Shear." *ACI Journal*, Vol. 83. No. 2, March-April 1986, pp. 219-231.

51. W.D. Cook and D. Mitchell. "Studies of Disturbed Regions Near Discontinuities in Reinforced Concrete Members." *ACI Journal*. March-April. 1988. pp. 206-216.

52. ACI Committee 318. "Building Code Requirements for Reinforced Concrete and Commentary." (ACI 318-89). American Concrete Institute. Detroit. 1989. p. 353.

53. CAN3 A23.3-M84. "Code for the Design of Concrete Structures for Buildings." Canadian Standards Association, Rexdale, Ontario. 1984, p. 281.

54. CEB-FIP, "Model Code for Concrete Structures," CEB, Paris, 1978.

55. N. Hawkins, A. Bao, and J. Yamazaki, "Moment Transfer from Concrete Slabs to Columns," *ACI Journal*, Vol. 86, No. 6, November-December, 1989, pp. 705-716.

56. M.E. Abdel-Razek. "Effect of Concrete Strength on the Behaviour of Slab-Column Connections Subjected to Monotonic and Cyclic Loading," Ph.D. Thesis, Cairo University, Egypt, 1994.

Appendix A

Computer Spreadsheet Program "PUNCH"

(Equations verification and examples)

PUNCHING SHEAR OF CONCRETE SLABS USING STRUT-AND-TIE METHOD

Input the following slab information:

TRIAL: Marzouk and Hussein, HS10, [36]

Square Column Dimen , c=	305 mm	fy rebar=	472 Mpa
Equiv. Circular Col. Diameter, B=	388 3 mm	p tens face=	0 0060
Dist. of Contraflexure, r3=	1700 mm	Es=	200000 Mpa
Structural Depth, d=	133 mm	Crack ang, O=	30 degrees
f'c=	22 7 Mpa		

SYMMETRIC PUNCHING

Width of critical section for flexure, b=B+3h= 827.3 mm
Depth of compression block, a=0.85*As*fy/[(0.85)*0.6f'c*b]= 27.7 mm
Depth of compression zone y=a/(0.85)=but >0.33h= 52.1 mm

CRACK ZONE OF STM

Crack zone length, L=(d-y)/sin0= 161.7 mm
Estimated Crack load, T=ft*L/3*(pi*(B+2(y+y1)/tan0)= 267.2 kn

where... ft=tensile capacity of concrete= 2.38 Mpa
=0.5*sqrt(f'c) when f'c<40Mpa
=0.05*(f'c) when f'c>40Mpa
y1=L/3*sin0= 27.0 mm

ULTIMATE FAILURE ZONE OF STM

ULTIMATE PUNCHING SHEAR BASED ON STM
Pult STM=
sin(Ø)/2*(pi*(B+2y/tanØ)*0.5y*f2max*DE= 348.3 kn.

where....DE=depth effect factor= (h/lch)^-0.35= 1.50
when f'c< 40Mpa, lch=500, when f'c >40Mpa lch=250
f2max=f'c/(0.8+170(0.002/tan^2(0))) = 19.3 Mpa
but >0 85*f'c

INTERACTION EQUATION FOR NONSYMMETRIC PUNCHING

c1=c2= 305 0 mm
Jc=d(c1+d)^3/6+(c1+d)d^3/6+2d(c2+d)[(c1+d)/2]^2= 5.81E+09
Tv=1-{1+.66*sqrt[(c1+d)/(c2+d)]}^-1= 0 40

Moment strength of Slab. Found when Vo is =zero
Mo=vc*Jc/(.5*(c1+d))*1/Tv= 126.4 kn-m
where vc=0 4sqrt(f'c)= 1 91 Mpa

MOMENT RESISTANCE DUE TO SHEAR=
Tv Mo= 50.6 kn-m/meter

MOMENT RESISTANCE DUE TO BENDING=
Considering effect of compression steel.....
assume p'= 0.002
A's= 220.1 mm^2 As= 660.2 mm^2
Mrb=(As-A's)fy(d-a/2)+A'sfy(d-d')= 34.0 kn-m/width of crit sect
=B+3h= 827.3 mm
Mrb= 41.0 kn-m/meter

TOTAL MOMENT RESISTANCE of SLAB=
Mult= 91.6 kn-m/meter

Pult STM = 348.3 kn ..... from STRUT-AND-TIE MODEL
Eccentricity,e=
130.0 mm

Allowable Axial load,P= 233.1 kn

PUNCHST2

Appendix B

Calculation Method for Punching Shear of Slab with Shear Reinforcement

Basis of Strut-and-Tie Model for Punching Strength of Concrete Slabs with Shear Reinforcement

- Cl 11.4.7.7 states that in regions of radiating compression struts (fan-shaped), the concrete compressive stress limits of Cl 11.4.7.3 and 11.4.7.5 may be considered satisfied by satisfying only the requirements of Cl 11.4.7.6 (b) and (c). Since Cl 11.4.7.6 (b) is not applicable, only Cl 11.4.7.6 (c) is required.

- Cl 11.4.7.6 (c) states that the compressive stress limits of all components of the strut-and-tie model in Figure 4.11 are satisfied if the tension reinforcement is anchored over a sufficient width that the tension results in a stress at the top node of less than $0.75\phi_c f'c$.

- P_{eq} assumed to act $d/2$ from last shear reinforcing element.

- Crack failure patterns indicate various angle cracks for different specimen, however, they always meet at the bottom node.

- Therefore, the failure mechanism was assumed to be at bottom node due to high concrete stress. however, the top node check was also done.

- Height of bottom node is assumed to be approximately equal to the compression depth of slab.

$$y = \frac{\phi s A s f y}{\phi_c 0.85 f'c \cdot b}$$